BIG BEND UNIT 4
THERMAL MIXING ZONE
VALIDATION STUDY

TAMPA ELECTRIC COMPANY
Tampa, Florida

June 14, 1984

BIG BEND UNIT 4
THERMAL MIXING ZONE
VALIDATION STUDY

TAMPA ELECTRIC COMPANY
Tampa, Florida

June 14, 1984

EXECUTIVE SUMMARY

This document describes the hydrothermal modeling conducted for the Tampa Electric Company (TEC) Big Bend Unit 4 thermal mixing zone validation, as required by the Conditions of Certification contained in the Florida Power Plant Site Certification Final Order (PA-79-012) and the National Pollutant Discharge Elimination System (NPDES) permit (No. FL0000817).

The Big Bend Station is located on the eastern shore of Hillsborough Bay near the juncture with Tampa Bay. All units at the Big Bend Station use once-through cooling. Water is withdrawn from an intake canal north of the plant and discharged to a canal located south of the facility. When Unit 4 begins operation, the total flow will be 2,148 cfs. The design maximum temperature rise across the Unit 4 condenser will be 16.8°F, which is the same as Units 1 through 3.

The CAFE-1/DISPER-1 models, which were developed at the Massachusetts Institute of Technology, were used to validate the size of the Big Bend Unit 4 thermal mixing zone. CAFE-1 simulates a coastal water body as 2-dimensional and homogeneous in density. Using input parameters, including boundary geometry, bathymetry, bottom roughness, tidal fluctuation, and wind, the model simulates surface elevations and depth-averaged currents varying in time and space.

The open-water boundary condition for the Big Bend model was determined by running, with the same tide and wind conditions, a second large element CAFE-1 model that covered all of Tampa Bay, a technique known as model "nesting."

DISPER-1 is designed as a companion to CAFE-1. Using the velocity fields generated by CAFE-1 as its fundamental input data, DISPER-1 solves the depth-averaged equations for mass balance of a passive constituent. In this application, the constituent is temperature.

Vertical profiles of dye concentrations and temperature obtained during the Aquatec, Inc. (1979) study show that the thermal plume from Big Bend Station quickly stratifies outside the discharge canal.

Therefore, DISPER-1 was modified to reflect the fact that the Big Bend thermal plume mixes over a limited depth. The realistic surface temperature, rather than the depth-averaged temperature, was used in calculating the surface heat exchange and mixing zone areas.

The Big Bend CAFE-1/DISPER-1 models were calibrated by the adjustment of specific parameters until field observations could be reproduced realistically during several calibration time periods. The models were then verified by comparing model results to a different independent data set.

Comparison of observed and predicted plumes indicates that the model tends to overpredict the plume area by 3 to 5 percent. Errors in reproducing individual plumes are random, and the typical error is 25 percent. The areas of larger plumes, simulated under extreme conditions, are predicted more accurately than the smaller plumes, with typical random errors of about 18 percent expected.

The calibrated and verified model was used to predict thermal mixing zone area for 10 combinations of receiving water, meteorological, and power plant operating conditions (scenarios). The scenarios were designed to focus on extreme conditions which would tend to maximize thermal mixing zone area, while bracketing the range of conditions anticipated. Under typical environmental and discharge conditions, the thermal mixing zone area ranged from 1,200 to 2,900 acres. The largest thermal mixing zone area predicted under any of the extreme conditions was 4,539 acres, which is less than the prescribed permit condition of 4,980 acres. Thus, this study validates the size of the permitted mixing zone.

TABLE OF CONTENTS

LIST OF TABLES

LIST OF FIGURES

LIST OF FIGURES
(Continued, Page 2 of 2)

1.0 INTRODUCTION

1.1 PROJECT HISTORY

Tampa Electric Company (TEC) currently is constructing Big Bend Unit 4, a 417-megawatt (MW) (net) capacity, coal-fired steam electric generating plant at the existing Big Bend Station in Hillsborough County, Florida. Construction of Big Bend Unit 4 began in November 1981, and commercial operation is scheduled for March 1985. The existing Units 1, 2, and 3 began operation in 1970, 1973, and 1976, respectively.

On August 1, 1980, TEC submitted to the U.S. Environmental Protection Agency (EPA) and the Florida Department of Environmental Regulation (DER) a 316 Demonstration Report, which assessed the impacts on Tampa Bay of condenser cooling water withdrawals and discharges resulting from the combined operation of Units 1 through 4. The assessments presented in the 316 Demonstration Report were based, in part, on results of mathematical modeling. Although the CAFE-1 and DISPER-1 models were considered appropriate for this study, a controversy developed during the review process over procedures and assumptions used in formulation, setup, and calibration of the near-field model. Consequently, the DER Site Certification Recommended Order was approved and adopted by the Governor and Cabinet on August 17, 1981, with the following Condition of Certification:

> The instantaneous zone of thermal mixing for the cooling system shall not exceed an area of 4,980 acres. The temperature at the point of discharge into Tampa Bay shall not be greater than 109 degrees F. The temperature of the water at the edge of the mixing zone shall not exceed the limitations of Paragraph 17-3.05(1)(d). The permittee shall validate the size of this mixing zone by submission of a verified or calibrated thermal dispersion model at least six months prior to commencement of operation. The Department and TECO shall agree to a program for selecting, verifying, and utilizing an appropriate model.

Similarly, EPA tentatively determined that the impact of the thermal discharge from Unit 4 is within acceptable limits under Section 316(a) of the Clean Water Act of 1977. The NPDES permit for Big Bend Units 1

through 4 (No. FL0000817) contains the following condition:

> The permittee shall validate the area to be impacted by the thermal plume from Units 1 through 4 by submitting a verified thermal dispersion model at least six months prior to commencement of operation of Unit 4. EPA, the State, and TECO shall agree to a program to ensure an appropriate model is selected, verified, and utilized.

In accordance with the above requirements, TEC submitted to DER and EPA, for review and comment, a plan of study describing the program to be followed in validating the Big Bend Unit 4 thermal mixing zone. TEC met with both agencies to review and discuss the proposed plan of study. Following these meetings, the agencies' comments were incorporated into a final plan of study submitted to both DER and EPA in March 1984. The final plan of study was accepted by both agencies.

1.2 OBJECTIVE AND APPROACH

The project objective, as defined by the Conditions of Certification and the National Pollutant Discharge Elimination System (NPDES) permit, was to verify the size of the thermal mixing zone associated with the operation of Big Bend Units 1 through 4 by submitting the results of a calibrated and verified hydrothermal model. To meet this objective, the numerical models CAFE-1 and DISPER-1 were used. The DISPER-1 model was modified to simulate the conditions found at Big Bend Station and thoroughly tested prior to calibration. The models were set up to simulate the Hillsborough/Tampa Bay system in the vicinity of Big Bend Station. Next, the models were calibrated and verified following procedures described in the Plan of Study (TEC, 1984).

Data required to set boundary conditions and data required for calibration and verification were obtained from existing sources, as discussed in Section 2.0 of this document. After the models were calibrated and verified, they were used to validate the size and extent of thermal mixing zone from Big Bend Units 1 through 4, as defined by the ambient +2°F isotherm for summer conditions and ambient +4°F isotherm for the remainder of the year [Chapter 17-3.05(1)(d), Florida Administrative Code (FAC)]. To validate the mixing zone size, 10 scenarios, defined by a combination of seasonal, plant operation, wind, and tide conditions, were modeled. All pertinent aspects of the model calibration/ verification and the mixing zone validation are presented in the remaining sections of this report.

1.3 THE SITE

The Big Bend Station is located on the eastern shore of Hillsborough Bay near the juncture with Tampa Bay (see Figures 1-1 and 1-2). All units at the Big Bend Station use once-through cooling. Water is withdrawn from an intake canal north of the plant and discharged to a canal located south of the facility. Each unit normally pumps 537 cubic feet per second (cfs) of cooling water. Thus, the three existing units pump, in total, 1,611 cfs of water. When Unit 4 begins operation, the total flow will be 2,148 cfs. The design maximum temperature rise across the Unit 4 condenser will be 16.8°F, which is the same as Units 1 through 3.

The Tampa Bay estuary is generally shallow, vertically well mixed, and has limited freshwater inflows. The tides are mixed, with significant energy in both diurnal and semi-diurnal components. The diurnal tidal range in Hillsborough Bay is about 2.8 feet (ft) [National Oceanic and Atmospheric Administration (NOAA), 1984], while tidal current velocities in the vicinity of the Big Bend Station are about 0.5 foot per second (ft/sec) (Aquatec, Inc., 1979).

Freshwater inflows are primarily through the Hillsborough, Alafia, Little Manatee, and Manatee Rivers. Since the total freshwater inflow is less than 0.3 percent of the tidal exchange (TECO, 1980), river discharges have little effect on the absolute magnitude of the bay currents, although they will have an impact on net circulation. Since the thermal load from the power plant is dissipated to the atmosphere within a time frame of a few days, net circulations due to river flows are not important from the standpoint of the hydrothermal modeling. Due to the size (346 square miles) and limited depth (mean depth 11 ft) of the bay, wind stress can have a significant impact on circulation, especially near the head of Tampa Bay.

Data collected during the 316 studies (TECO, 1977) show ambient water temperatures near the Big Bend Station are about 30°C in the summer and 12°C in the winter. Salinities near the power plant vary from 21 parts per thousand (ppt) to 27 ppt, averaging 24 ppt.

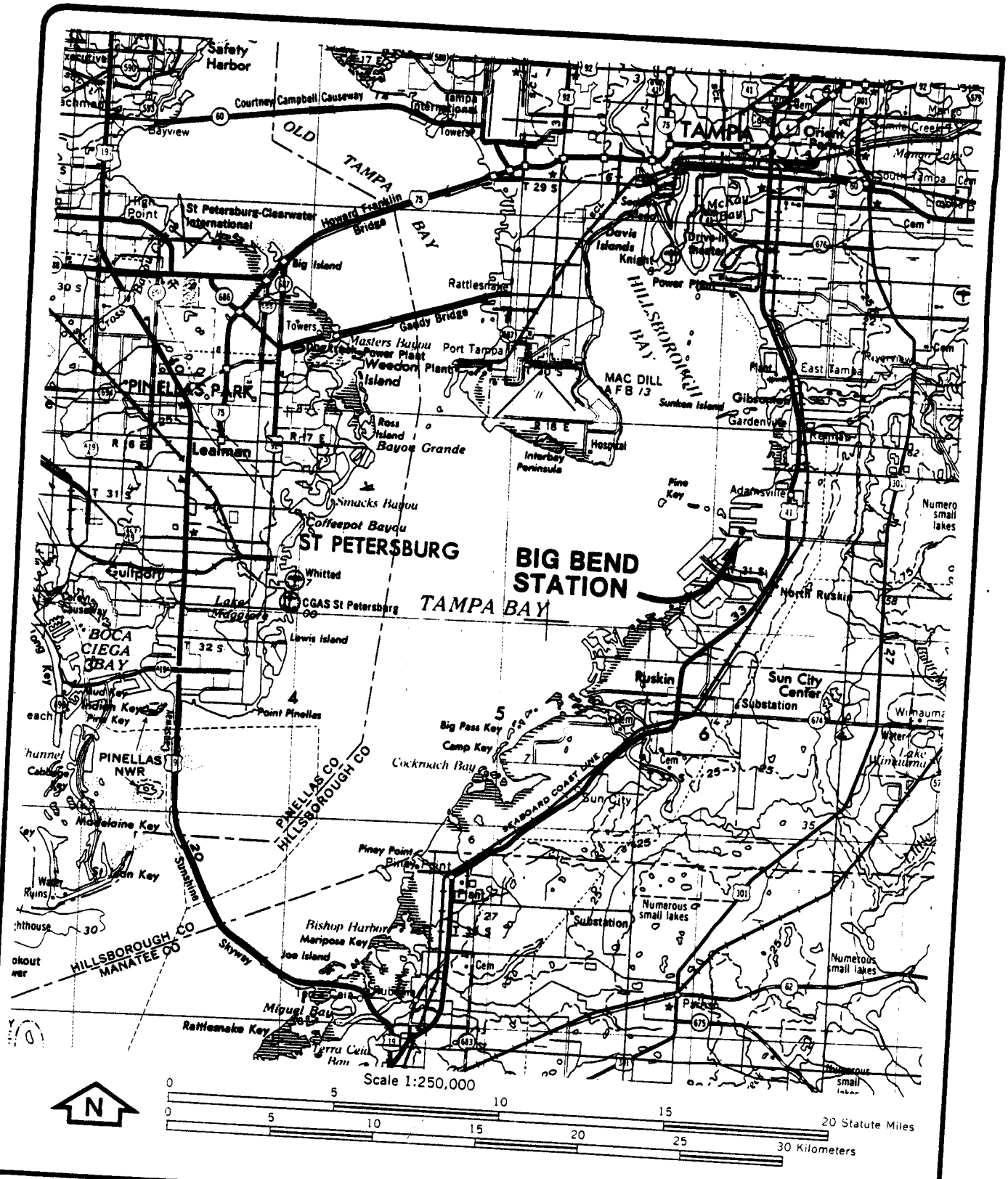

Figure 1-1
REGIONAL LOCATION MAP

SOURCE: ESE, 1984.

TAMPA ELECTRIC COMPANY

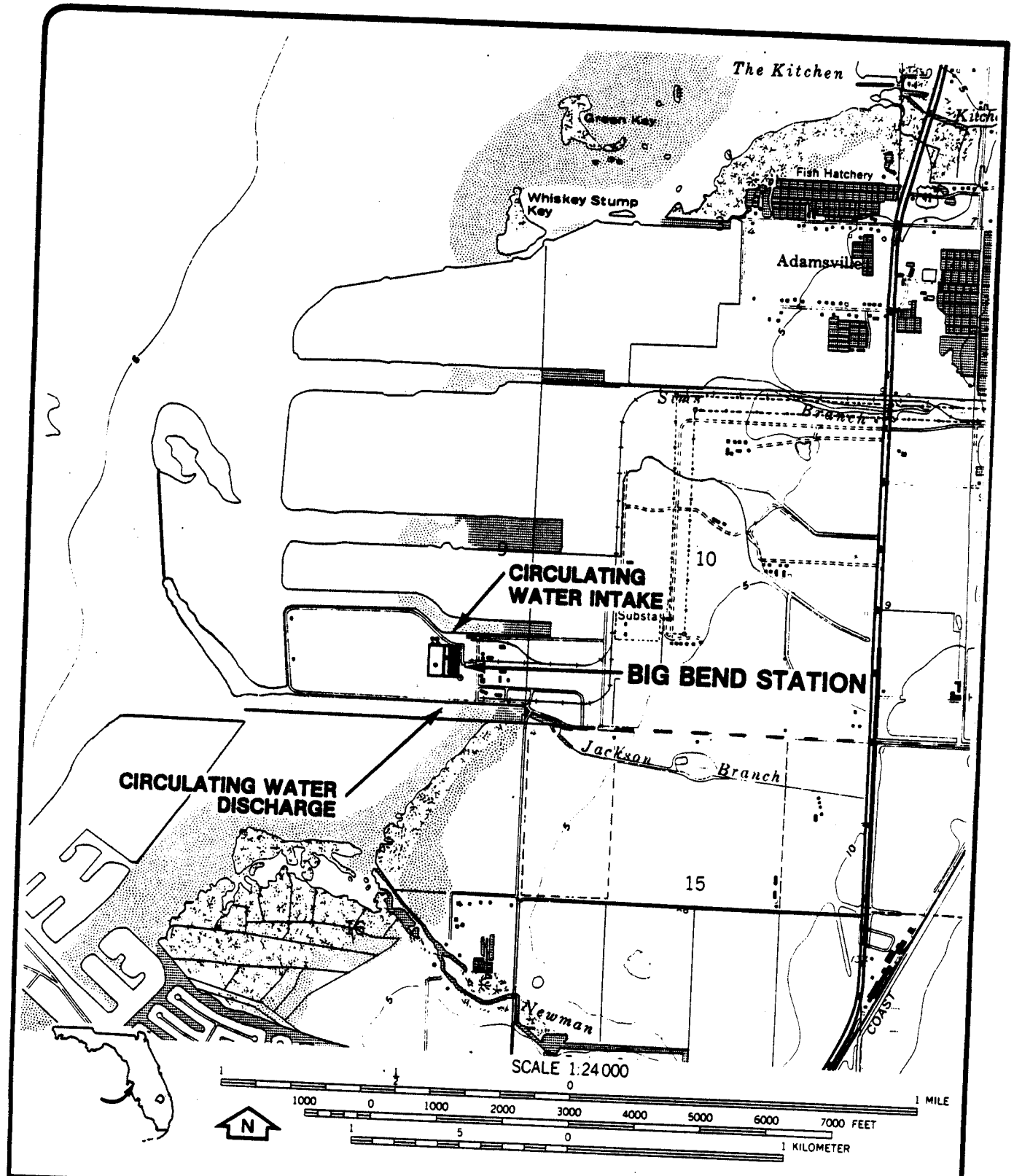

Figure 1-2
GENERAL SITE LOCATION

SOURCE: ESE, 1984.

TAMPA ELECTRIC COMPANY

2.0 DATA SOURCES

In preparing the plan of study, careful consideration was given to the quality and availability of data required to develop, calibrate, and verify the model. It was concluded that available data were adequate to perform the mixing zone validation study. The data sources used in the modeling effort are discussed in the following paragraphs.

Bathymetric Data--The bathymetry of Tampa Bay was determined from National Ocean Survey (NOS) nautical charts and boat sheets and from recent verification of Tampa Bay bathymetry conducted by Camp Dresser and McKee (CDM) under contract with DER.

Meteorological Data--Air temperature, dew point temperature, and wind data at Tampa International Airport were available from the U.S. National Climatic Center.

Big Bend Operational Data--The Big Bend Station condenser water flow and temperature, the intake temperature, and the water temperature at the end of the discharge canal for the calibration and verification time periods were provided by TEC. The projected flows, the design maximum and normal temperature increases across the condensers, and the seasonal ambient temperatures and salinities were obtained from the 316 Demonstration Report (TECO, 1980).

Current Data--During October 1979, two current meters were deployed by Aquatec, Inc. (1979); one of these was located within the modeled region, as shown in Figure 2-1. The current meter was deployed 2 meters (m) below the surface in 6 m of water. Data were recorded every 15 minutes.

Dye Studies--Aquatec, Inc. (1979) also conducted a dye dispersion study during October 1979 in which dye was released continuously from the discharge canal. The results of this study are contour plots of surface dye concentrations at high slack, strength of ebb, low slack, and strength of flood for two complete tidal cycles. Also, at selected

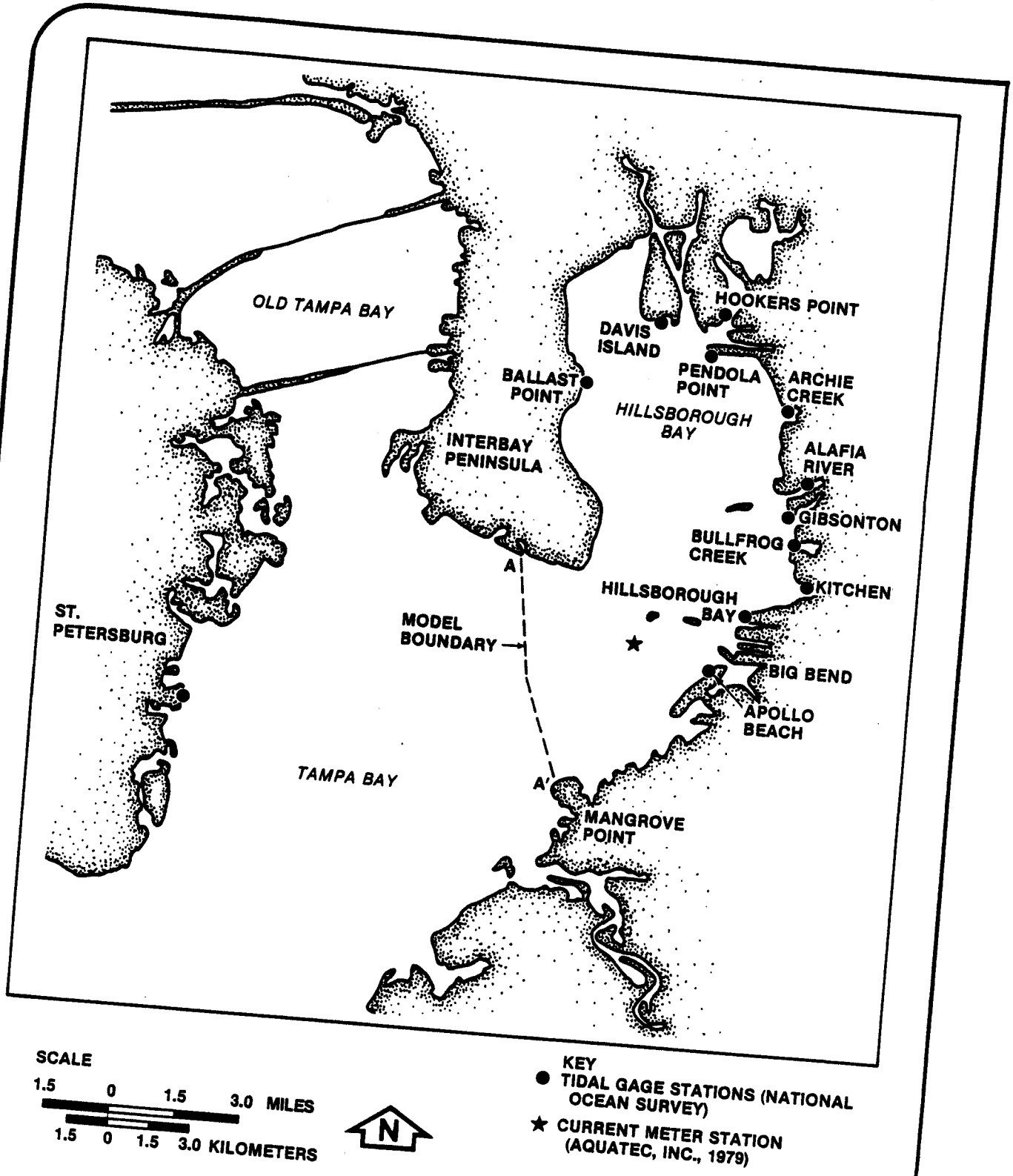

Figure 2-1
TIDE AND CURRENT METER STATIONS

SOURCE: ESE, 1984.

TAMPA ELECTRIC COMPANY

locations throughout the plume, vertical profiles of dye concentrations and temperature were plotted. These vertical profiles were used to establish the plume depth of mixing.

Thermal Infrared Surveys--During November 1979, the EPA Environmental Monitoring Systems Laboratory conducted four aerial thermal infrared surveys (Divers, 1980). The first infrared plate was acquired at low tide (16:38 EDT, November 14, 1979). The second plate was at a strength of flood (8:51 EDT, November 15, 1979). The third and fourth plates were at high tide (13:28 EDT, November 17, 1979) and strength of ebb (15:53 EDT, November 17, 1979). The first two plumes are separated in time from the last two plumes by more than 2 days. During this time period, the half-life of heat in the bay, based on the calibrated heat exchange coefficient, was 12.5 hours. Therefore, the last two plumes are thermodynamically independent of the first two plumes.

Tide Data--Time series water-level fluctuations in 1979 at several stations in Hillsborough Bay were computed using the St. Petersburg tidal record and transfer functions developed from data collected simultaneously at all stations in 1977.

During 1977, 11 tide gages were operated in Hillsborough Bay (see Figure 2-1). The recording periods of these gages are shown in Table 2-1. The closest primary tide station is at St. Petersburg, Florida. Data from this gage were obtained for the periods shown in Table 2-1. Water levels at each of these stations were recorded hourly in 1977.

During the period in 1979 in which the dye study and thermal infrared surveys were conducted, no gages were operated in Hillsborough Bay.

To calibrate the hydraulic and thermal plume dispersion models, transfer functions were established to predict the tides at the Hillsborough Bay stations based on the tides at St. Petersburg.

Table 2-1. Available Tide Data for Model Calibration

NOS Station No.	Location (Florida)	Recording Period	Breaks in Data
872 6537	Apollo Beach	3/3/77-6/30/77	
872 6562	Hillsborough Bay	3/9/77-6/30/77	
872 6572	The Kitchen	3/8/77-10/18/77	7/17/77-7/19/77
872 6587	Bullfrog Creek	1/13/77-4/30/77	1/31/77-2/1/77
872 6602	Gibsonton		2/10/77-2/14/77
872 6609	Alafia River	3/17/77-8/26/77	
872 6632	Archie Creek	1/1/77-5/2/77	
872 6639	Ballast Point	1/1/77-5/2/77	
872 6651	Pendola Point	1/1/77-7/30/77	4/17/77-4/18/77
872 6657	Davis Island	3/1/77-8/3/77	
872 6668	Hooker Point	1/1/77-3/31/77	
872 6520	St. Petersburg	1/1/77-3/29/77	
872 6520	St. Petersburg	1/1/77-10/31/77	
		9/1/79-12/31/79	

Source: National Ocean Survey.

These transfer functions were developed using harmonic analysis of the 1977 tide data. The transfer functions then were used to reconstruct the water-level time series in Hillsborough Bay during 1979, using the 1979 St. Petersburg tide data.

The tide data at each of the Hillsborough Bay stations were determined as follows:

1. St. Petersburg 1977 tide data were harmonically analyzed to compute the phases and amplitudes of the five diurnal and semi-diurnal tide components, as shown in Table 2-2. The residual water-level fluctuation was then computed by subtracting the diurnal/semi-diurnal tidal components from the complete tide data record.

   This process can be expressed mathematically as:

$$\eta_{sp} = \sum_{i=1}^{5} a_{sp,i} \cos(\omega_i t - \sigma_{sp,i}) + R_{sp} \qquad (2\text{-}1)$$

   where: η_{sp} = the water-level elevation at St. Petersburg,
   $a_{sp,i}$ = amplitude of the i^{th} component,
   ω_i = frequency of the i^{th} component,
   $\sigma_{sp,i}$ = phase of the i^{th} component, and
   R_{sp} = residual at St. Petersburg.

2. The same procedure is applied to the 1977 tide data from the tide stations in Hillsborough Bay. Similarly, the tide data can be expressed as:

$$\eta_j = \sum_{i=1}^{5} a_{j,i} \cos(\omega_i t - \sigma_{j,i}) + R_j \qquad (2\text{-}2)$$

$j = 1 \ldots, 11$

Table 2-2. Diurnal and Semi-Diurnal Tides

Tidal Component	Period (Hours)
M_2	12.4206
K_1	23.9345
S_2	12.0000
O_1	25.8193
N_2	12.6583

Source: Dronkers, J.J. 1964. "Tidal Computations in Rivers and Coastal Waters."

where: η_j = water level at the j^{th} gage in Hillsborough Bay,

$a_{j,i}$ = amplitude of the i^{th} component at the j^{th} gage,

ω_i = frequency of the i^{th} tidal component,

$\sigma_{j,i}$ = phase of the i^{th} component at the j^{th} gage, and

R_j = residual of the j^{th} gage.

3. The transfer functions were expressed as:

$$\eta_j = \sum_{i=1}^{5} C_{j,i}\, a_{sp,i} \cos(\omega_i t - \sigma_{sp,i} - \Delta_{j,i}) + R_{sp} \qquad (2\text{-}3)$$

$j = 1, 2, \ldots, 11$

where: $C_{j,i} = \dfrac{a_{j,i}}{a_{sp,i}}$, and

$\Delta_{j,i} = \sigma_{j,i} - \sigma_{sp,i}$

This analysis assumes that the residuals at all gages, including the St. Petersburg gage, are the same. The results of the harmonic analysis and tide transformation indicated that the tide data at Davis Island and Hooker's Point were too short to provide an accurate tidal function. The residuals of the tide data at the Kitchen, Hillsborough Bay, Bullfrog Creek, Alafia River, and Archie Creek gages were not the same as the St. Petersburg residual because these gages are influenced by stream discharge and local boundary effects. The residuals at the selected four remaining gages in Hillsborough County were nearly identical. Therefore, the transfer functions could be used to reconstruct tide data in 1979 at Apollo Beach, Gibsonton, Ballast Point, and Pendola Point. The transfer coefficients for these stations are given in Table 2-3.

Table 2-3. Transfer Coefficients

	Apollo Beach (j=1)	Gibsonton (j=2)	Ballast Point (j=3)	Pendola Point (j=4)
$C_{1,j}$	1.215	1.136	1.153	1.280
$C_{2,j}$	1.122	1.009	1.053	1.101
$C_{3,j}$	1.230	1.226	1.223	1.291
$C_{4,j}$	1.019	0.970	1.049	1.070
$C_{5,j}$	0.965	1.149	1.382	1.230
$\Delta_{1,j}$*	-0.169	-0.085	0.442	-0.094
$\Delta_{2,j}$	-0.264	0.094	0.460	-0.157
$\Delta_{3,j}$	0.021	-0.089	0.537	-0.079
$\Delta_{4,j}$	-0.283	0.028	0.374	-0.101
$\Delta_{5,j}$	-0.598	-0.382	0.476	-0.200

* $\Delta_{i,j}$ in hours.

Source: ESE, 1984.

4. The harmonic analysis was conducted using St. Petersburg 1979 tide data. The amplitude ($a_{sp,i}$), phase ($\sigma_{sp,i}$), and the residual (R_{sp}) were computed. The harmonic coefficients are shown in Table 2-4.

5. Using the transfer coefficients established in Step 3 (Table 2-3) and the values for St. Petersburg from Step 4 (Table 2-4), the tide data at the four Hillsborough gages were computed for 1979.

Table 2-4. Results of the Harmonic Analysis of St. Petersburg Tide Data in 1979

Period (hours)	Amplitude (m)	Phase (degrees)
12.4206	0.5884	278.96
23.9345	0.4309	80.56
12.0000	0.1846	56.53
25.8193	0.4077	76.13
12.6583	0.0927	203.16

Source: ESE, 1984.

3.0 MODEL DESCRIPTIONS AND FORMULATIONS

3.1 CAFE-1/DISPER-1 MODELS

The CAFE-1/DISPER-1 models, which were developed at the Massachusetts Institute of Technology, were used to validate the size of the Big Bend Unit 4 thermal mixing zone. These models were selected for the following reasons:

1. The models are "state of the art" and are able to account for all significant hydrologic forces in the Tampa Bay system (tides, wind stress, and freshwater inflow).
2. The models use a finite-element numerical scheme. This permits the use of small-scale elements (approximately 250 ft) near the discharge to define the plume, while large-scale elements can be used away from the study area to define the boundary conditions.
3. The finite-element scheme allows complex bathymetric and basin geometrics to be represented more accurately.
4. The models were used on previous Big Bend studies, and both the agencies and third party reviewers found the models appropriate for the Tampa Bay/Big Bend system.
5. Finally, the CAFE-1/DISPER-1 system is a reliable model, having been calibrated and verified in many coastal embayments, including Massachusetts Bay, Narragansett Bay (Leimkuhler et al., 1975; Pearce and Christodoulou, 1975; Wang and Connor, 1975), and Biscayne Bay (Wang, 1978). The success of CAFE-1/DISPER-1 in reproducing field results in these applications leads to a high degree of confidence in its ability to reasonably simulate the effects of the Big Bend thermal discharge. The model has also been recently applied to Chesapeake Bay and Apalachicola Bay (Wang, 1983).

CAFE-1 simulates a coastal water body as 2-dimensional and homogeneous in density. Using input parameters, including boundary geometry, bathymetry, bottom roughness, tidal fluctuation, and wind, the model simulates surface elevations and depth-averaged currents varying in time

and space. The model is based on vertically integrated equations for conservation of mass and momentum which are applicable for shallow nonstratified bodies of water, such as Tampa Bay. The model solves these equations based on the finite-element technique. In this technique, the water body is subdivided into a finite number of triangular sections (finite elements). Within each of these elements, the solution of the conservation equations is approximated, leading to estimates of flow and water level at the vertices (grid points). Since each vertex belongs to two or three elements, the solution in one element affects adjacent elements, leading to a large number of simultaneous equations whose solution results in a continuous, gradually varying spatial field of velocity vectors and water level.

The finite element method for solving the equations may be contrasted with the finite difference method in which the grid is rectangular and the mass and momentum equations are approximated, rather than the elemental solution as in the finite element approach. Both techniques solve the same set of hydrodynamic equations. The chief advantage of the finite element technique is that the size and orientation of the elements can vary throughout the region being modeled. This feature permits better resolution of the flow field in regions of special interest, such as the locale of a thermal discharge, as well as a more accurate representation of complex boundaries with fewer grid points. Accurate simulation with fewer grid points is important in reducing computer core storage requirements and computation, and data preparation cost.

The derivation and specification of the hydrodynamic equations used by CAFE-1 are presented by Wang and Connor (1975) and summarized in Appendix A to the Big Bend Station--Unit 4, 316 Demonstration report (TECO, 1980) and will be only briefly reviewed here. The fundamental assumptions are:

1. Water is incompressible and homogeneous in density,
2. Hydrostatic equilibrium is maintained, and
3. Reynolds stresses are represented by the eddy viscosity concept.

Further, the equations are integrated over depth to yield the vertically averaged volocities at any location. These equations, as presented by Pritchard (1971), are technically valid for a well-mixed estuary such as Tampa Bay. Tidal forcing, wind stress, and bottom friction are all accounted for in the CAFE-1 model.

Boundaries are of two types, discharge boundaries and force boundaries. At the shoreline, discharge is set to zero; at stream mouths, the Big Bend discharge canal, or the condenser water intake canal, the discharge is specified (nonzero). Force boundaries are those at the bay mouth or the model boundary where the tidal forcing (water level versus time) is specified.

Initial conditions (flow and water level) must be specified at all nodes. However, prior knowledge of these conditions is not required, since the transient caused by an error in the specification of the initial conditions will dissipate quickly within the modeling of a few tidal cycles.

DISPER-1 is designed as a companion to CAFE-1. Using the velocity fields generated by CAFE-1 as its fundamental input data, DISPER-1 solves the equation for mass balance of a passive constituent. In this application, the constituent is temperature. A technically more accurate term is enthalpy, which is proportional to temperature at constant pressure and within a limited temperature range (e.g., $\pm 30°C$). The equation expressing the mass balance of a constituent in a fluid system is often referred to as the advection-dispersion equation. The principal assumption required to develop the equation is the representation of turbulent mixing processes by the standard eddy diffusion concept. DISPER-1 inputs include the eddy diffusion coefficients, CAFE-1 results for time-dependent velocities and water levels, bathymetry, temperature decay rate, and sources of heat (Big Bend discharge flow and temperature). DISPER-1, like CAFE-1, solves the vertically integrated

equation. The model formulation is provided in detail by Leimkuhler et al. (1975) and TECO (1980) and is not repeated here.

As with all 2-dimensional (i.e., single layer) models, CAFE-1/DISPER-1 is not able to calculate explicitly the vertical profile of temperature within the thermal plume itself or the resultant density stratification. As far as circulation is concerned, the effect of this limitation is minor. Ambient currents in the vicinity of the mixing zone result from the interaction of tidal currents and wind stress acting in concert through the whole bay system, as well as the effects of the discharge itself. The depth-averaged effects of the intake and discharge are appropriately accounted for within CAFE-1. In context of these dominant circulation-forcing phenomena, all of which are effectively simulated by CAFE-1, any secondary features induced by vertical stratification should be relatively minor.

This is not the case with surface heat flux. Since the depth-averaged temperature is less than the surface temperature when the plume is stratified, the original model formulation requires use of an artificially high heat exchange coefficient to simulate correctly the surface heat flux and to calibrate the model. Under these conditions, the heat exchange coefficient is no longer based on physical principles, and extrapolation to new conditions can be questionable. To avoid this potential source of uncertainty, DISPER-1 was modified to account for the effects of vertical stratification on surface heat exchange within the plume. The thermal stratification of the Big Bend plume and the program modifications incorporated in DISPER-1 to account for this phenomenon are discussed in the following sections.

3.2 THERMAL STRATIFICATION

Vertical profiles of dye concentrations and temperature obtained during the Aquatec, Inc. (1979) study show that the thermal plume from Big Bend Station quickly stratifies outside the discharge canal. The depth to which the plume stratifies, or the depth of mixing, d_m, is defined as follows:

$$d_m = \int_0^H \frac{(T(z)-T_a)}{(T_s-T_a)}\, d_z \quad \text{(for temperature)} \tag{3-1}$$

$$d_m = \int_0^H \frac{C(z)}{C(z=0)}\, d_z \quad \text{(for dye)} \tag{3-2}$$

where: z = the distance from the water surface,
H = the total depth of the water column,
$T(z)$ = the vertical temperature profile,
T_a = the ambient water temperature,
T_s = the surface temperature, and
$C(z)$ = the vertical dye profile.

The depth of mixing was calculated for 57 profiles. The area-weighted average depth of mixing over the plume equaled 1.5 m, with a standard deviation of 0.35 m. The depth of mixing was greatest at the point of discharge (2.7 m), but stabilized quickly to 1.5 m within a few hundred feet of the point of discharge.

In general, the depth of mixing will be controlled by the densimetric Froude number at the point of discharge, although wind can play a role in determining the mixing depth if the depth of mixing is small or the winds strong. To evaluate the relative importance of these two mechanisms in controlling the Big Bend plume, the densimetric Froude number at the point of discharge and the correlation coefficient between wind speed

and depth of mixing were calculated. The densimetric Froude number at the point of discharge equaled 0.91, which is close to the critical value of 1.0. On the other hand, the correlation coefficient between wind and depth of mixing equaled 0.13, which is statistically insignificant. These results strongly suggest the densimetric Froude number at the point of discharge controls the depth of mixing and that wind mixing is not important. For this reason, densimetric Froude number similarity was used to determine the depth of mixing for all calibration and verification simulations and for all modeled scenarios. The depth of mixing is given by:

$$d_m = d_m' \left(\frac{Q}{Q'}\right)^{2/3} \left(\frac{\beta'}{\beta}\right)^{1/3} \qquad (3\text{-}3)$$

where: $\beta = \frac{\Delta\rho}{\rho} = 1 - \text{EXP}\ (-\alpha\ \Delta T)$,

$\frac{\Delta\rho}{\rho}$ = the density difference between the warm and cold water layers,

Q = the discharge flow rates,

α = the coefficient of thermal expansivity, and

ΔT = the excess temperature at the point of discharge.

Prime symbols refer to conditions during the dye study,
therefore, $d_m' = 1.5$ m,

$Q' = 30.3\ m^3/sec$, and

$\Delta T' = 5.0°C$.

The DISPER-1 model was modified to incorporate the effects of thermal stratification and the depth of mixing parameter. These modifications are discussed in Section 3.3.

3.3 PROGRAM MODIFICATIONS

Two modifications were made to the CAFE-1/DISPER-1 models. The first modification involved a simple change in the input/output format to facilitate quality assurance on the project. The second modification involved changing the DISPER-1 model to account for the effects of thermal stratification.

In accordance with the quality assurance section of the plan of study, the CAFE-1 and DISPER-1 programs were modified to rewrite the input data of each run on the output listing. This allowed the inputs and outputs of each computer run to appear on the same printout. This modification had no effect on the operation of the models or their results.

The DISPER-1 program was modified to improve simulation of the thermal plumes. Prior to modification, all DISPER-1 internal calculations were based on the depth-averaged excess temperature, which was also the final output of the model. Nevertheless, permit conditions are based on excess surface temperature. Furthermore, to calibrate the model using realistic heat exchange coefficients, the heat loss must be based on surface excess temperature, not depth-averaged excess temperature. To address this, DISPER was modified to represent the surface excess temperature as a function of the depth-averaged excess temperature and the depth of mixing. The modified program was thoroughly tested prior to implementation in this study and found to produce the intended effects, with no effect on mass conservation.

Figure 3-1 illustrates the basis of the modification. Actual vertical thermal profiles in the thermal plume are similar to the solid line profile shown in Figure 3-1. The dashed line is the vertical temperature profile effectively modeled by DISPER-1 before the modification, while the dotted line profile is the modified version. All three profiles have the same vertically averaged excess temperature and thus the same heat content. In addition, the modified profile (dotted line) also has the same excess surface temperature as the actual plume.

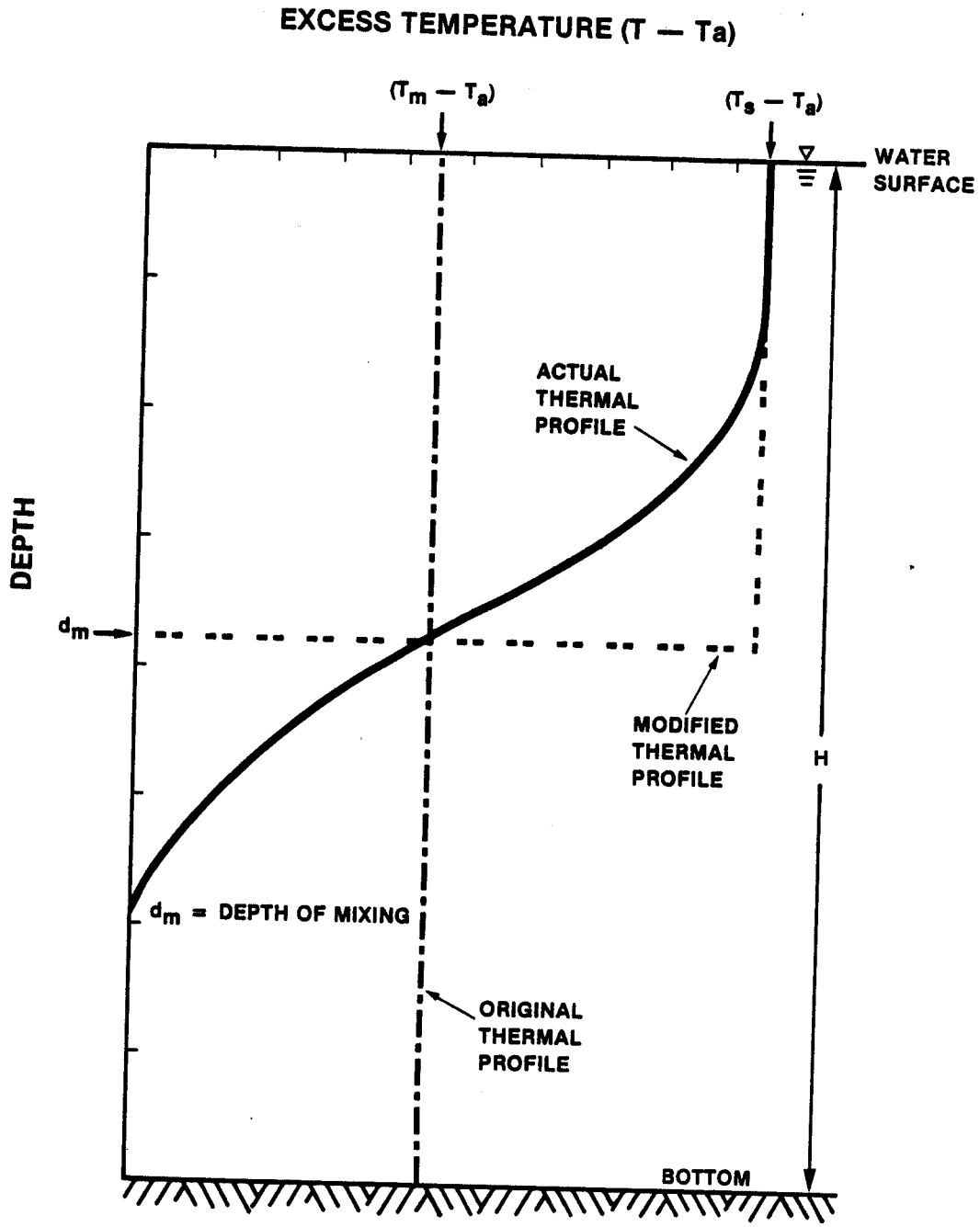

Figure 3-1
DISPER-1 THERMAL PROFILE MODIFICATION
SOURCE: ESE, 1984.

TAMPA ELECTRIC COMPANY

The vertically averaged excess temperature (T_m-T_a) through the full depth of the water column, H, is the parameter internally calculated by DISPER-1. This vertically averaged excess temperature, $T_m - T_a$, can be defined in terms of depth of water column (H), excess surface temperature ($T_s - T_a$), and depth of mixing (d_m) using the following relationship:

$$(T_s-T_a) = (T_m-T_a) \frac{H}{\min (d_m,H)} \qquad (3\text{-}4)$$

where: $\min (d_m,H) = \begin{cases} H, \text{ if } H \leq d_m \\ d_m, \text{ if } d_m \leq H \end{cases}$

and

$$d_m = \int_0^H \frac{(T(z)-T_a)}{(T_s-T_a)} \, d_z \qquad (3\text{-}5)$$

where: $T(z)-T_a$ = the excess temperature versus depth.

In the modified version, Equation 3-4 is applied to calculate the surface excess temperature, which is reported as the final output and forms the basis for definition of the thermal mixing zone.

The depth of mixing concept is also used in calculating surface heat losses. The surface heat (enthalpy) flux is given by the following equation:

$$\text{Heat Flux} = K_e (T_s-T_e) \approx K_e (T_s-T_a) \qquad (3\text{-}6)$$

where: K_e = surface heat exchange coefficient (Watt/m^2/°C), and
T_e = the equilibrium temperature as defined by Edinger *et al.* (1974).

Usually, it can be assumed that the equilibrium temperature, T_e, is equal to the ambient temperature, T_a. The first-order decay rate constant for heat is defined as the ratio of the heat flux to the total amount of excess heat (excess enthalpy) in the water column.

Since the total excess heat in the water column can be expressed as:

$$\rho C_p H (T_m - T_e) = \rho C_p H (T_m - T_a) \qquad (3\text{-}7)$$

where: ρ = the density of water, 1,015 kg/m^3, and
C_p = the specific heat capacity of water, 4,092 W sec/kg°C.

then, the first-order decay rate for heat, k, is:

$$k = \frac{K_e (T_s - T_a)}{\rho C_p (T_m - T_a) H} = \frac{K_e}{\rho C_p \min (d_m, H)} \qquad (3\text{-}8)$$

The DISPER-1 subroutine DECAY has been modified to reflect the above. The input parameter controlling surface heat loss is $K_e / \rho C_p$, or $2.41 \times 10^{-7} K_e$, with K_e in Watt/m^2/°C units.

In summary, DISPER-1 has been modified to reflect the fact that the Big Bend thermal plume mixes over a limited depth. The realistic surface temperature, rather than the depth-averaged temperature, is used in calculating the surface heat exchange and in output listings.

3.4 NODE AND ELEMENT STRUCTURE

The first step in the modeling process is to segment the modeled domain into a series of nodes and elements. The geometry of the segmented model should accurately represent the geometrics of the system. The water depth is specified at each nodal point.

The Big Bend CAFE-1/DISPER-1 model was set up to include all of Hillsborough Bay, with an open-water boundary extending from the Interbay Peninsula south to a point near Mangrove Point on the east side of Tampa Bay (see Figure 2-1). This modeling domain was selected for the following reasons:

1. By incorporating all of Hillsborough Bay, only one open-water boundary was required. This eliminated the difficult task of synchronizing two open-water boundaries.
2. The open-water boundary is sufficiently south and west of the Big Bend zone of discharge that small errors in boundary conditions will not influence the mixing zone, and the largest plumes will fall within the modeled area.

Figure 3-2 shows the node and element structure used in the model. Elements with length scales of about 250 ft were used in the neighborhood of the discharge to provide the necessary spatial resolution. Small elements were also used to accurately represent channels between the islands located northwest of the Big Bend discharge canal. Away from these areas, where spatial resolution is not required, element sizes were increased to minimize the already considerable computer storage requirements.

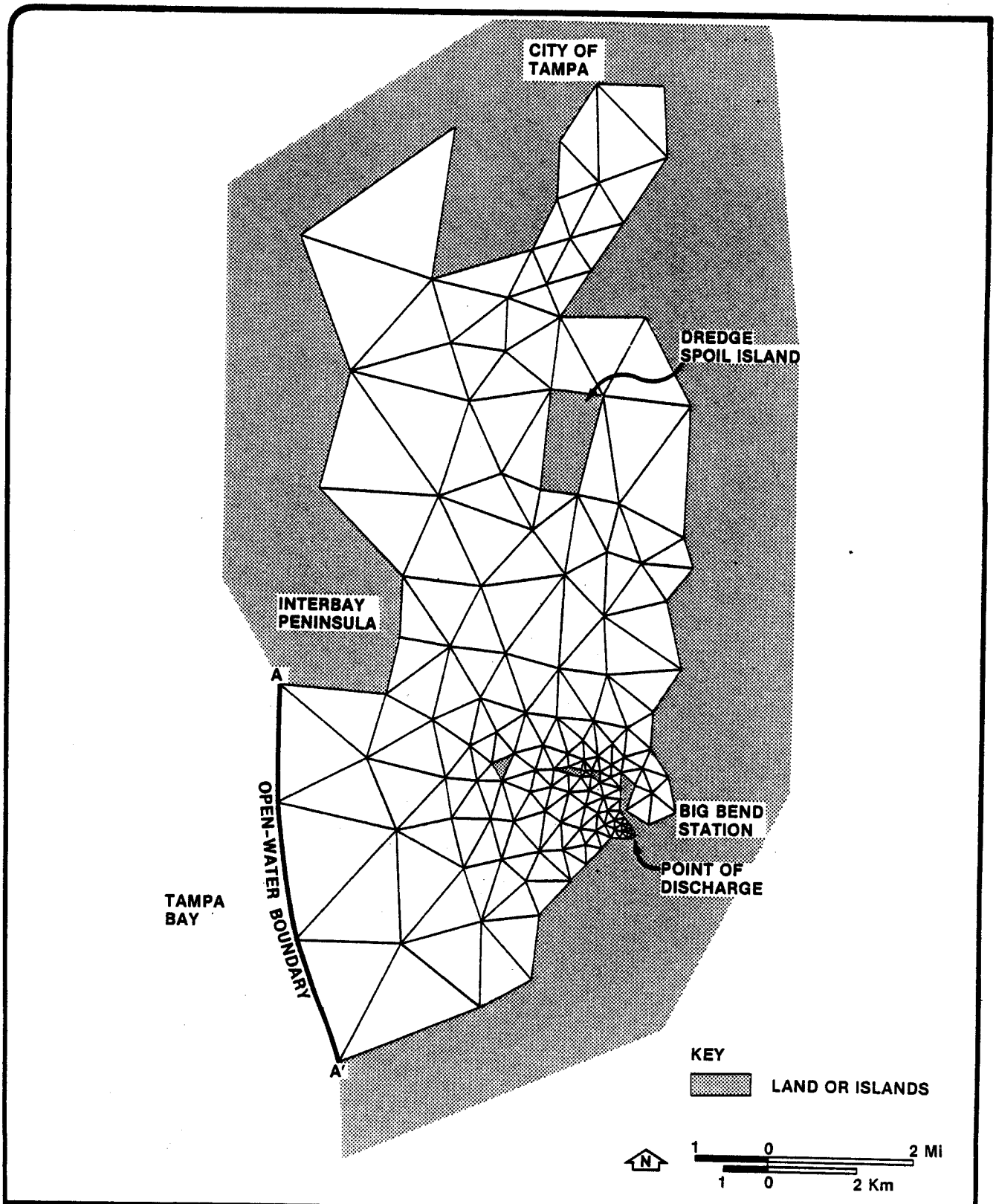

Figure 3-2
NODE AND ELEMENT STRUCTURE FOR BIG BEND CAFE-1/DISPER-1 MODELS

SOURCE: ESE, 1984.

TAMPA ELECTRIC COMPANY

3.5 BOUNDARY CONDITIONS

To drive the model, boundary conditions must be specified as a function of time. Water levels must be specified at the open-water boundary, and flow rates and temperatures specified at the point of discharge.

The model boundary in the vicinity of the Big Bend discharge canal is the bayward extension of the canal, where water temperature is continuously monitored. These temperature data were used during model calibration and verification to specify the thermal boundary conditions for DISPER-1. This removed the need to calculate heat dissipation in the discharge canal, which was significant during this period due to lower flows and high heat exchange rates. Under four unit operations and with more typical heat exchange rates, heat loss in the discharge canal is minor and, therefore, was neglected.

The open-water boundary condition for the Big Bend model was determined by running, with the same tide and wind conditions, a second large element CAFE-1 model that covered all of Tampa Bay (see Figure 3-3). The water levels predicted by the large element CAFE-1 model are then used to set the boundary conditions for the Big Bend model. This technique is known as model "nesting." The large element CAFE-1 model was calibrated and checked by comparing tidal amplitudes and phase relationships at several tidal stations in Hillsborough Bay. Tidal phases generally were accurate to 15 minutes, and the tidal amplitudes were reproduced to $\pm$10 percent. This degree of accuracy is sufficient for the large element model, considering the rigorous calibration and verification procedures followed on the Big Bend model.

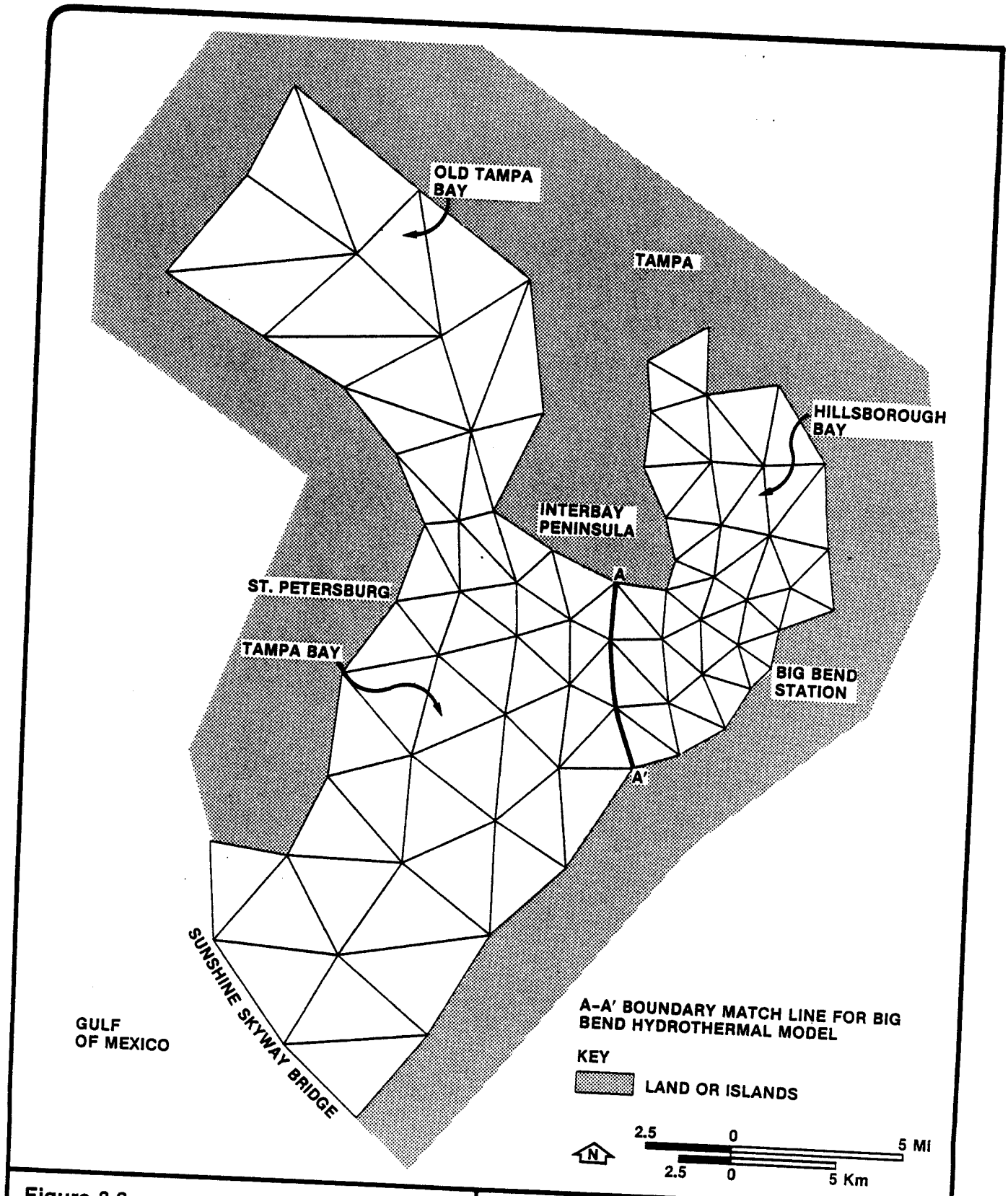

Figure 3-3
NODE AND ELEMENT STRUCTURE FOR THE LARGE ELEMENT CAFE-1 MODEL

SOURCE: ESE, 1984.

TAMPA ELECTRIC COMPANY

4.0 MODEL CALIBRATION AND VERIFICATION

The Big Bend CAFE-1/DISPER-1 models were calibrated by the adjustment of specific parameters until field observations could be reproduced realistically during several calibration time periods. The models were then verified by comparing model results to a different independent data set. The objective of the calibration process was to realistically simulate hydraulic and thermal dissipation conditions in Tampa Bay without recourse to unrealistic values of the calibration parameters. For example, numerous models of estuarine hydraulics have been calibrated by use of a Manning's n coefficient of 0.018 to 0.035. Use of values outside this range, except in localized areas, would not be justifiable. The need to use a value outside of this range could indicate that the roughness factor is being used to compensate other undiscovered errors in the model. This objective has been met, as will be demonstrated in the sections to follow.

The hydraulic model, CAFE-1, was calibrated and verified before proceeding with the calibration of the water quality model, DISPER-1. The calibration parameters for CAFE-1 are: Manning's n coefficient, which controls bottom friction; eddy viscosity; and the depth of water in the vicinity of the spoil disposal area and islands just north of the discharge canal, which was not known a priori. The calibration parameters for DISPER-1 are eddy diffusivity and surface heat exchange coefficient.

Eddy diffusivity and viscosity can be defined over broad ranges upon consideration of tidal energetics, bay dimensions, and grid dimensions from a variety of sources, including, but not limited to, Officer (1977), Bowden (1977), and Yudelson (1967). Heat exchange coefficient estimation procedures are provided by Edinger et al. (1974).

4.1 HYDRAULIC CALIBRATION

The hydraulic calibration period was October 10 and 11, 1979. During this period, tide and current meter data were available to compare with model results. The best comparison between predicted and observed values was found using Manning's n coefficient of 0.023 and an eddy viscosity of 25 m^2/sec. The eddy viscosity is consistent with values recommended by Fischer et al. (1979). The value of Manning's n is well within the range of values recommended by Chow (1959).

Use of these parameter values led to realistic simulation of water-level elevation and macroscale currents in Hillsborough Bay. Subsequent attempts to reproduce the observed dye plumes, however, indicated that although the macro-scale dynamics of Hillsborough Bay were well simulated, localized circulation patterns in the vicinity of the Big Bend discharge were not being simulated adequately. It was apparent from each of the eight observed near-field dye plumes, as well as the aerial infrared studies, that the Big Bend plume remained south of these islands. The model, on the other hand, carried significant concentrations of dye through these channels on the flood. Some of the dye remained trapped to the north of the larger islands on the ebb. Clearly flow through these channels is considerably more restricted in the prototype than in the model.

To resolve this, all available bathymetric data in the vicinity of these islands were reviewed carefully. This review showed that relatively little was known about bathymetry in these areas during the calibration/verification period. Since these areas are used for dredge spoil disposal, bathymetry may be expected to vary unpredictably. Therefore, if a bathymetric survey were conducted today, it would not

define the conditions during the calibration and verification period. Considering these factors, the best source of information on the hydraulic conveyance in this area is the dye plumes. The hydraulic conveyance had to be reduced enough to prevent significant dye intrusion on the flood. Depths were reduced from 5 ft below mean low water to 2 ft below mean low water. This change was consistent with aerial photographs taken in 1980 in which these areas appear very shallow. The Manning's n coefficient was increased from 0.023 to 0.05, which is consistent with reported values for disturbed areas (Chow, 1959). These changes reduced the flow through the island channels, but did not completely block the tidal flows.

The calibrated model results realistically simulate the large-scale dynamics of Hillsborough Bay, as indicated by Figures 4-1 through 4-4. Figures 4-1 through 4-3 show the comparison between actual and simulated water levels at Apollo Beach, Ballast Point, and Pendola Point, respectively. The "observed" water levels plotted in these figures are the water levels provided by the transfer functions discussed in Section 2.0. Figure 4-4 is a stick plot comparison of current vectors at the current meter south of Pine Key (see Section 2.0). The current meter record includes data points every 15 minutes, while model results were provided every hour. Predicted current speeds are slightly lower than observed, principally because the model-generated currents represent a depth average over 15 to 20 ft, while the current meter was at a depth of 2 m below the water surface. The characteristic logarithmic profile of current speed versus depth implies that the depth-averaged speed will be about 80 percent of the speed at 2 m. Currents observed at 2 m are also more strongly influenced by wind than the depth-averaged current, which could account for some of the variability in the observed currents as well as the occasional differences between observed and predicted directions. Overall, the agreement between observed and predicted tides and currents is good.

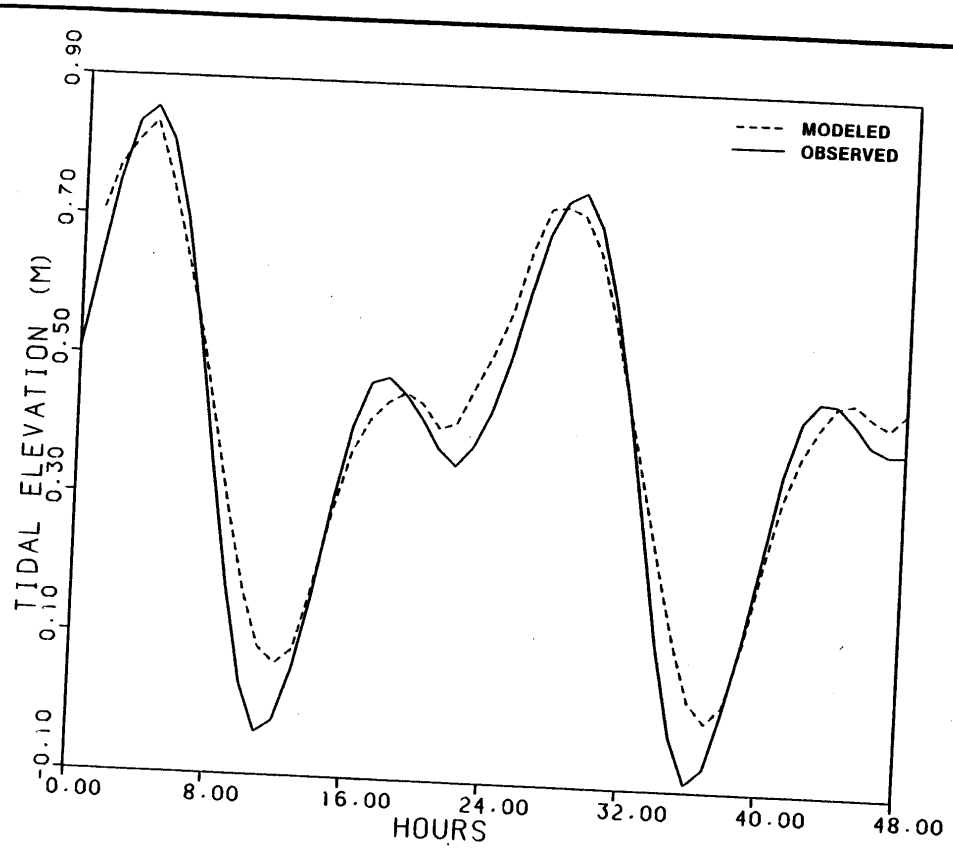

Figure 4-1
HYDRAULIC CALIBRATION: APOLLO, OCT. 10 - 11, 1979

SOURCE: ESE, 1984.

TAMPA ELECTRIC COMPANY

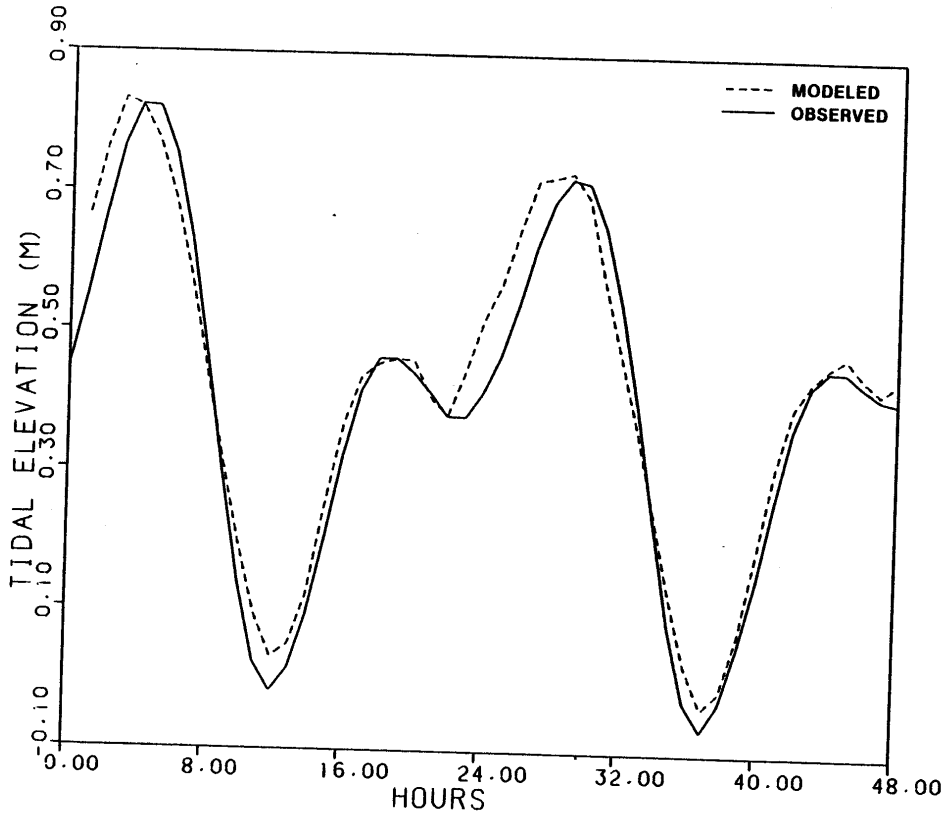

Figure 4-2
HYDRAULIC CALIBRATION: BALLAST, OCT. 10 - 11, 1979

SOURCE: ESE, 1984.

TAMPA ELECTRIC COMPANY

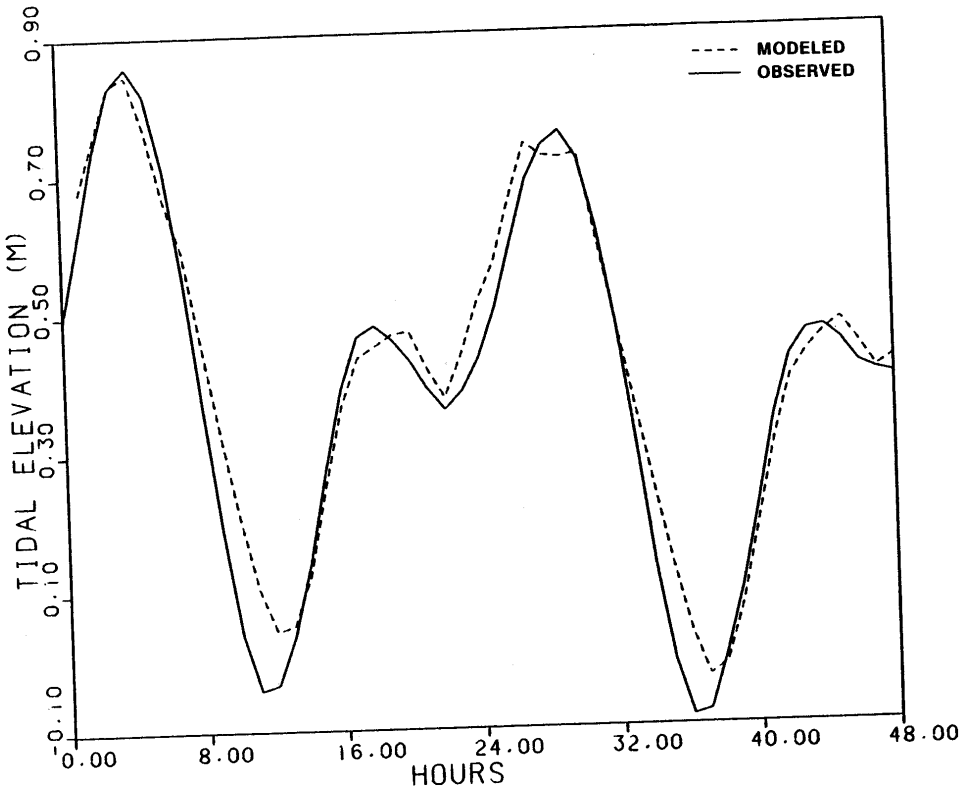

Figure 4-3
HYDRAULIC CALIBRATION: PENDOLA, OCT. 10 - 11, 1979.

SOURCE: ESE, 1984.

TAMPA ELECTRIC COMPANY

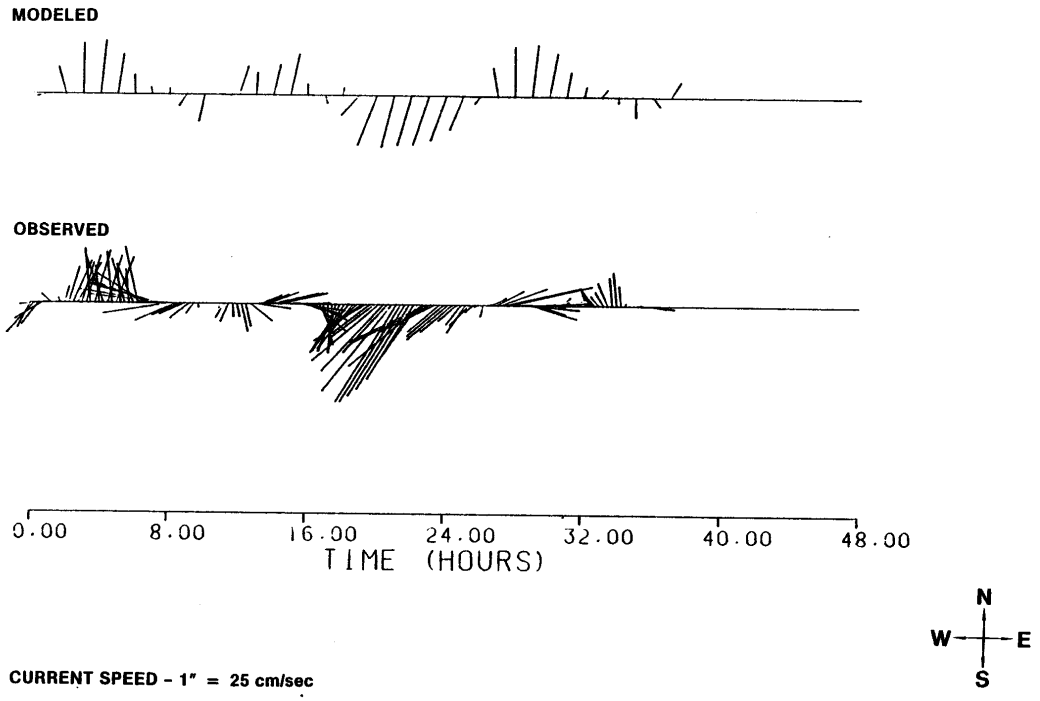

Figure 4-4
HYDRAULIC CALIBRATION: OCT. 10 - 11, 1979

SOURCE: ESE, 1984.

TAMPA ELECTRIC COMPANY

4.2 HYDRAULIC VERIFICATION

To verify that the CAFE-1 model can accurately predict a variety of hydraulic conditions, the calibrated model was used to simulate hydraulic conditions on October 16 and 17, 1979, during the dye study. Since this period was 5 days after the hydraulic calibration period, the flow conditions are independent of those observed during the calibration period. Tides were mixed during the calibration period, while the verification period exhibited a regular semi-diurnal tide. Winds were slightly stronger during the verification period and consistently from the northeast, while the wind direction during the calibration period was variable. In both cases, wind speeds were approximately equal to the typical wind speed of about 7 to 10 kts for the Tampa Bay area. Figures 4-5 through 4-8 illustrate the realistic simulation of water-level elevations and currents during the verification period.

Based on these results, it is concluded that the hydraulic model is calibrated and verified and provides a useful basis for thermal plume prediction.

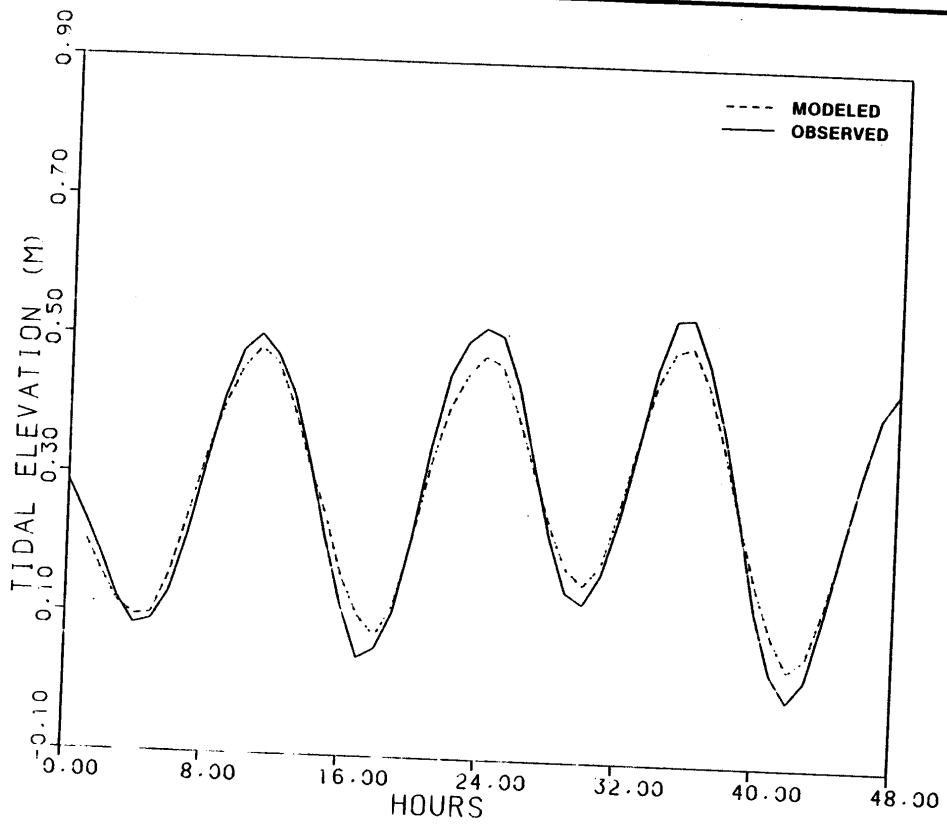

Figure 4-5
HYDRAULIC VERIFICATION: APOLLO, OCT. 16 - 17, 1979

SOURCE: ESE, 1984.

TAMPA ELECTRIC COMPANY

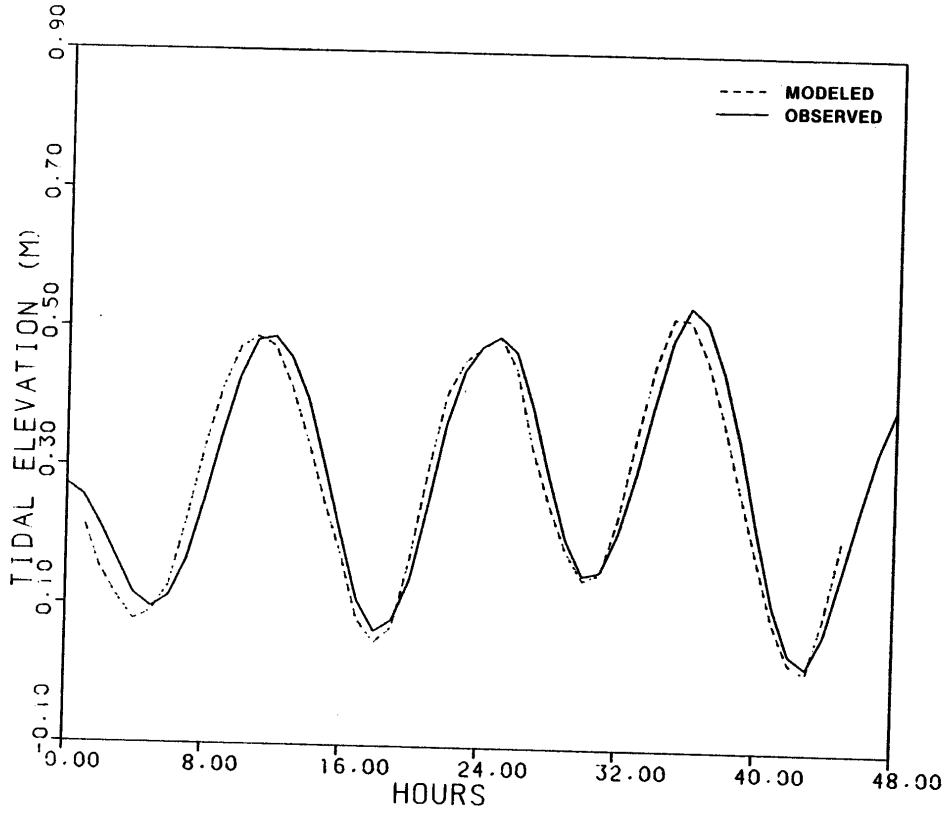

Figure 4-6
HYDRAULIC VERIFICATION: BALLAST, OCT. 16 - 17, 1979

TAMPA ELECTRIC COMPANY

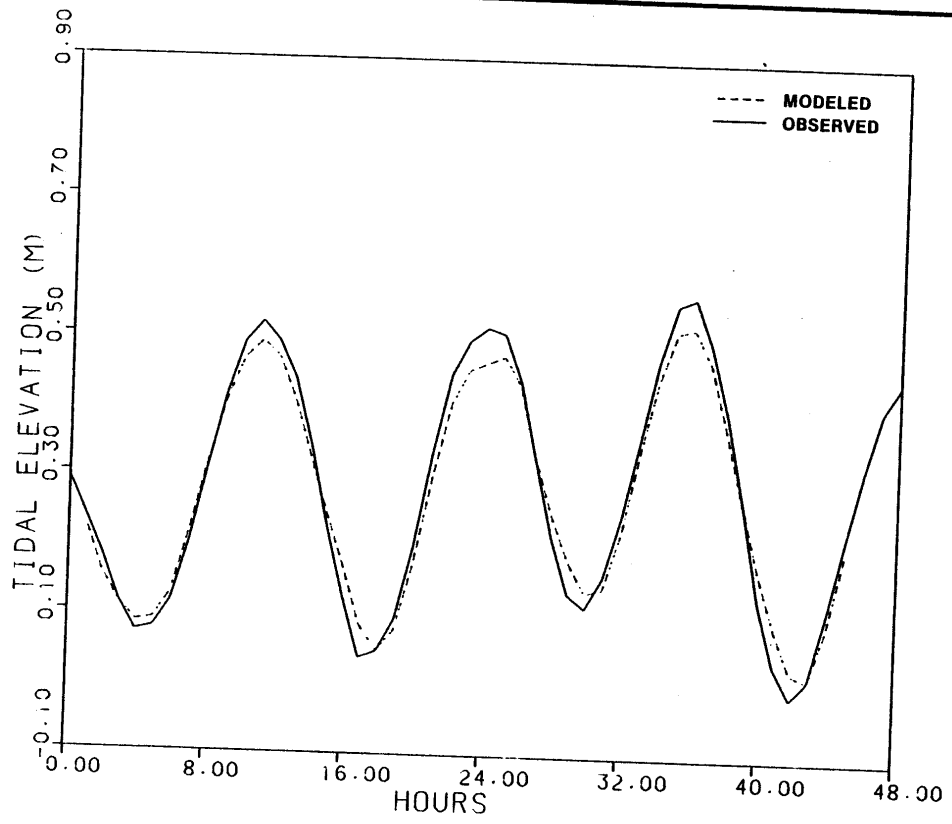

Figure 4-7
HYDRAULIC VERIFICATION: PENDOLA, OCT. 16 -17, 1979
SOURCE: ESE, 1984.

TAMPA ELECTRIC COMPANY

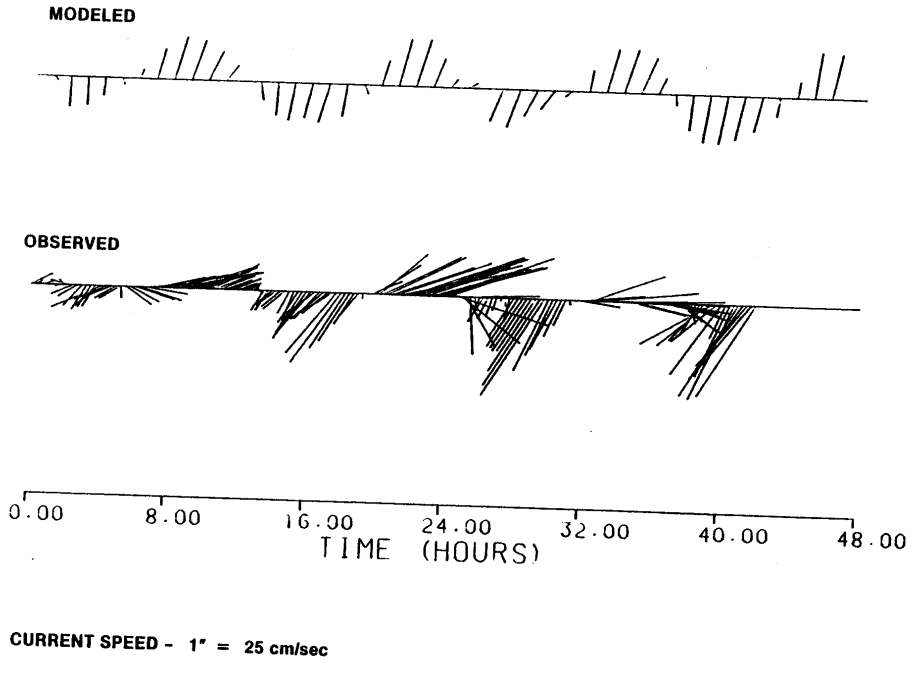

Figure 4-8
HYDRAULIC VERIFICATION: OCT. 16 - 17, 1979

SOURCE: ESE, 1984.

TAMPA ELECTRIC COMPANY

4.3 CALIBRATION OF THE DISPERSION COEFFICIENT

During October 16-17, 1979, a series of eight near-field dye plumes were measured by Aquatec, Inc. Two plumes were taken at each of the major phases of the tide. An initial attempt to simulate these plumes with an isotropic dispersion coefficient of 25 m^2/sec indicated that the actual dispersion rates were lower, and the dispersion process was anisotropic, with higher dispersion rates along the direction of flow and lower dispersion transverse to the flow. The actual plumes exhibited sharper dye concentration gradients and had a more elongated jet-like appearance than the predicted plumes. Attempts to reproduce the shape of the observed plumes using lower anisotropic dispersion coefficients, for example 10 m^2/sec in the longitudinal direction and 1 m^2/sec in the transverse direction, caused the model to become unstable after approximately 20 hours of simulation time. The instabilities originated in the larger elements, away from the point of discharge, and propagated back into the area of the discharge. Since the thermal plumes to be simulated under the projected scenario for four units at 100-percent capacity require simulation times of 250 hours to reach thermal equilibrium, such instabilities could not be tolerated.

Review of DISPER-1 stability criteria (Christodoulou *et al.*, 1976) clarifies the nature of the problem. Stability of the DISPER model is governed by multiple criteria. The simulation will be well behaved only within a range of parameter values defined by the following equations:

$$1.22\ U\ \frac{\Delta t}{\Delta S} + 8\ E\ \frac{\Delta t}{\Delta S^2} < 1 \qquad (4\text{-}1)$$

$$\frac{E_x + E_y}{(u + v)\Delta S} > \frac{1}{6} \qquad (4\text{-}2)$$

where: E = the vector magnitude of the longitudinal and transverse dispersion coefficients, $\vec{E}_x + \vec{E}_y$;

U = the magnitude of the velocity in the critical element;

ΔS = the length scale of the critical element; and

Δt = the time step; and

u, v = the magnitude of the x-component and y-component velocities, respectively.

The first condition implies that the maximum time step is established by the smallest elements (when ΔS is small, the left-hand side of the inequality is large). The second condition implies that the largest elements in the grid limit the size of the dispersion coefficient. Large elements with appreciable tidal velocities demand large dispersion coefficients to maintain stability in the concentration (temperature) predictions. This relationship is independent of time step, so a reduction in time step will not enhance stability. Therefore, the only way to reduce the dispersion coefficient while maintaining stability would be to reduce the largest element size. Such a reduction was not feasible for the following reasons. Small elements were required near the point of discharge to resolve the dynamics of the discharge. Furthermore, the boundaries of the model must be far enough away to contain the "worst-case" plumes to be simulated during operation of four units. Therefore, a significant reduction in the size of the largest elements would dictate a proportional increase in the number of elements. This could not be done, even on the University of Florida's powerful computing system, due to storage limitations.

In consideration of these factors, several tests were conducted to determine the lowest set of anisotropic dispersion coefficients which could be used while maintaining model stability. The minimum dispersion coefficients were found to be: 40 m^2/sec in the longitudinal direction and 10 m^2/sec in the transverse direction. Although these values are within the range of values appropriate for estuarine systems, they were still too large to accurately reproduce the shapes of the dye plumes. The predicted plumes are broader and more radial in shape than the observed plumes, which are more jet-like in appearance with sharper

transverse gradients. Nevertheless, areas within specific concentration isopleths were reproduced adequately. The nature of the difference in shape between predicted and observed plumes is also reflected in the thermal plumes of the calibration and verification period.

4.4 THERMAL CALIBRATION

During November 14 through 17, 1979, a series of four aerial infrared photographs of the Big Bend thermal plume was taken by EPA (Divers, 1980). The first two, taken on November 14 and 15, were selected as the basis for calibration of the heat exchange coefficient. Surface temperatures are indicated in these photographs as bands of color in 0.5°C increments. To provide a calibration "target," the areas experiencing a surface temperature increase of 1°C over intake temperature were determined by planimetry from the aerial photographs. Hourly flow and temperature data provided by TEC were used to define loading rates at the model boundary during the calibration and verification time period.

The rate of surface heat loss from a heated plume is most sensitive to wind speed and dew point temperature. Dependence on wind speed is parameterized, according to the method of Edinger et al. (1974), via the surface heat exchange coefficient, while the dependence on dew point temperature is incorporated into both the heat exchange coefficient and the equilibrium temperature. Equations describing the heat exchange are given below:

$$\frac{DT}{Dt} = -K_e (T_s - T_e) / \rho C_p h \qquad (4\text{-}3)$$

where: T = the vertically averaged water temperature,
T_s = the water surface temperature,
t = time,
K_e = the surface heat exchange coefficient,
ρ = the density of water,
C_p = the heat capacity of water,
h = the depth of water through which the heat is lost, and
T_e = equilibrium temperature.

The equilibrium temperature, Te, is given by:

$$T_e = T_d + \frac{S}{K_e} \qquad (4\text{-}4)$$

where: T_d = the dew point temperature, and
S = the incoming solar radiation.

The heat exchange coefficient is determined from a nomograph (Figure 2.4.2 of Edinger et al., 1974) and varies with the water temperature, dew point temperature, and wind speed.

In modeling, it is usually assumed that the ambient water temperature, T_a, is the equilibrium temperature, T_e. In a large body of water, such as Tampa Bay, this assumption is not always valid. The thermal calibration data were taken during the first "winter" weather pattern of 1979. For the week preceding November 13, the dew point temperature was consistently above 14°C, averaging about 18°C to 20°C. On the morning of November 13, the dew point temperature began to decline steadily from 20°C, reaching 5°C at the time of the first aerial infrared flyover on the afternoon of November 14. Wind conditions during this period were similar to long-term average winds at 8 to 12 kts.

During the thermal calibration period, the dew point temperature averaged 6.5°C. The incoming solar radiation was approximately 160 W/m^2, and the wind speed was 5.2 m/sec (10 kts). From Edinger et al. (1974), the heat exchange coefficient for these conditions would be 35 $W/m^2/°C$. Thus, the equilibrium temperature from Equation 4-4 would be:

$$T_e = 6.5 + \frac{160}{35} = 11.1°C = 52°F$$

However, during this same period, the ambient temperature was 70° to 75°F, significantly higher than the equilibrium temperature. Under these

conditions, the Edinger coefficient must be adjusted to account for the difference between equilibrium temperatures and ambient temperature. This adjustment is calculated as follows.

In modeling a thermal plume, the model simulates the excess temperature, or the temperature above ambient temperature. As an initial condition, the excess temperature (or model temperature) is set to zero everywhere in the bay, except the discharge point which is assigned an excess temperature. The discharge flow carries the increment of temperature (heat) into the bay system where it is advected, dispersed, and dissipated. Thus, the model describes heat losses by the following equation:

$$\frac{D(T_s - T_a)}{Dt} = -K_m \frac{(T_s - T_a)}{\rho C_p d_m} \qquad (4\text{-}5)$$

where: K_m = the heat exchange coefficient used by the model,
T_a = a constant ambient temperature or a "reference temperature," and
d_m = the depth of mixing (see Equation 3-2).

In the prototype (Tampa Bay), the temperature dynamics can be expressed by:

$$\frac{D(T_s - T_a)}{Dt} = \frac{DT_s}{Dt} - \frac{DT_a}{Dt} = \frac{-K_e}{\rho C_p}\left[\frac{(T_s - T_e)}{d_m} - \frac{(T_a - T_e)}{H}\right] \qquad (4\text{-}6)$$

where: H = the average depth of the bay.

For the model to simulate the plume realistically, Equation 4-5 must equal Equation 4-6; thus:

$$K_m \frac{(T_s - T_a)}{\rho C_p d_m} = \frac{K_e}{\rho C_p}\left[\frac{T_s - T_e}{d_m} - \frac{T_a - T_e}{H}\right] \qquad (4\text{-}7)$$

or

$$K_m = \frac{K_e\, d_m}{T_s - T_a} \left[\frac{T_s - T_e}{d_m} - \frac{T_a - T_e}{H} \right] \qquad (4\text{-}8)$$

During the calibration period, the following values were determined from the data sources:

K_e = 35 W/m^2/°C, T_s = 25.7°C, T_a = 24°C, T_e = 11.1°C, d_m = 1.5 m, and H = 1.9 m.

The surface temperature given above is a representative surface temperature over the entire plume in the region having $\Delta T > 1$°C. This temperature is calculated by the following equation:

$$T_s = T_a + \frac{(T_o - T_a) + 1}{2} \qquad (4\text{-}9)$$

where: T_o = the temperature at the point of discharge, T_o = 26.5°C; and

H = the average depth of the bay in the area of the plume.

Applying these values to Equation 4-8 for K_m, the model heat exchange coefficient must be 2.6 times the Edinger heat exchange coefficient, or 91 W/m^2/°C. Use of this value is equivalent to using the Edinger coefficient, since the ambient temperature is not at equilibrium. Stated another way, if the model could be calibrated with an input K_m = 91 W/m^2/°C, it would imply that the Edinger coefficient is precisely valid in Tampa Bay.

The model was run for the period November 13 through 15, 1979, setting K_e = 35 W/m^2/°C as recommended by Edinger. Table 4-1 presents the predicted areas within the 1°C isotherm and compares them with areas determined from the aerial infrared photographs. The model overestimated

the plume size by 14 percent on average, overestimating the size of the first plume by 39 percent. Based on these results, K_e was increased by 9 percent to 38 $W/m^2/°C$. Table 4-1 shows that the bias in average plume area was reduced to 7 percent, with the errors in individual plumes nearly symmetric (+25 percent and -20 percent). A further increase in K_e could have eliminated the bias altogether. However, a small "conservative" bias (prediction of slightly larger plumes than observed) should lead to an environmentally conservative estimate in prediction of thermal mixing zone size.

The shapes of the thermal plumes resulting from the calibrated model are shown in Figures 4-9 and 4-11. Corresponding observed plumes are shown in Figures 4-10 and 4-12. The predicted plumes illustrate the more radial shape resulting from excessive dispersion as discussed in Section 4.3. Plume shape may also be more strongly influenced by local winds in the prototype than in the model, since the model can not account for internal friction at the plume boundary.

Table 4-1. Calibration Results: Area Within $\Delta T > 1°$ C (Acres)

Observed Area		Predicted Area: Edinger Heat Exchange K_e = 35 W/m^2/°C Area (Variance from Observed)	Predicted Area: Calibrated K = 38 W m^{-2} C^{-1} Area (Variance from Observed)
October 14, 16:38 EDT, Low Tide	124	172 (+39%)	155 (+25%)
October 15, 8:51 EDT, Strength of Flood	98	84 (-14%)	78 (-20%)
AVERAGE	111	128 (+15%)	119 (+ 7%)

Source: ESE, 1984.

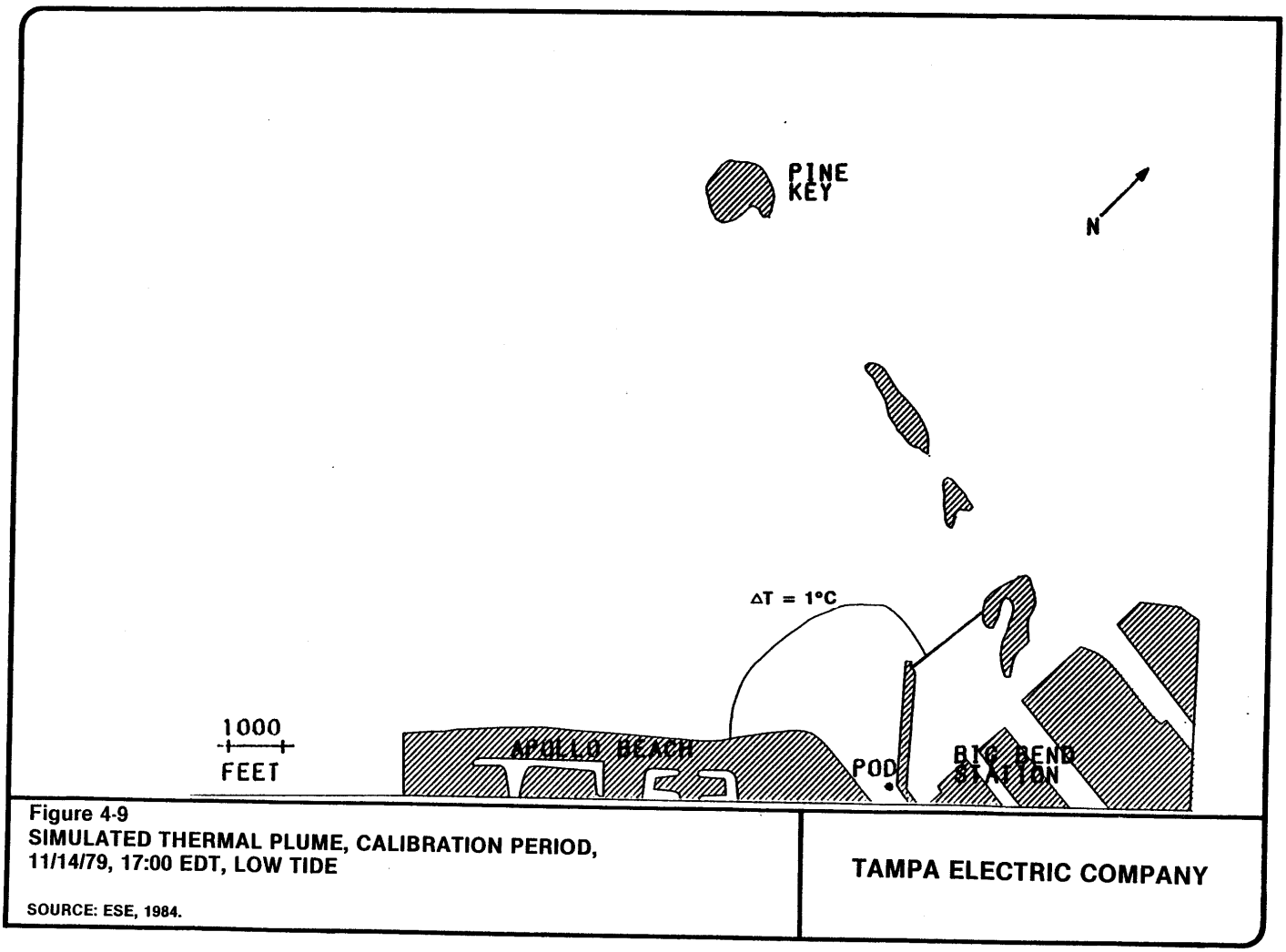

Figure 4-9
SIMULATED THERMAL PLUME, CALIBRATION PERIOD, 11/14/79, 17:00 EDT, LOW TIDE

SOURCE: ESE, 1984.

TAMPA ELECTRIC COMPANY

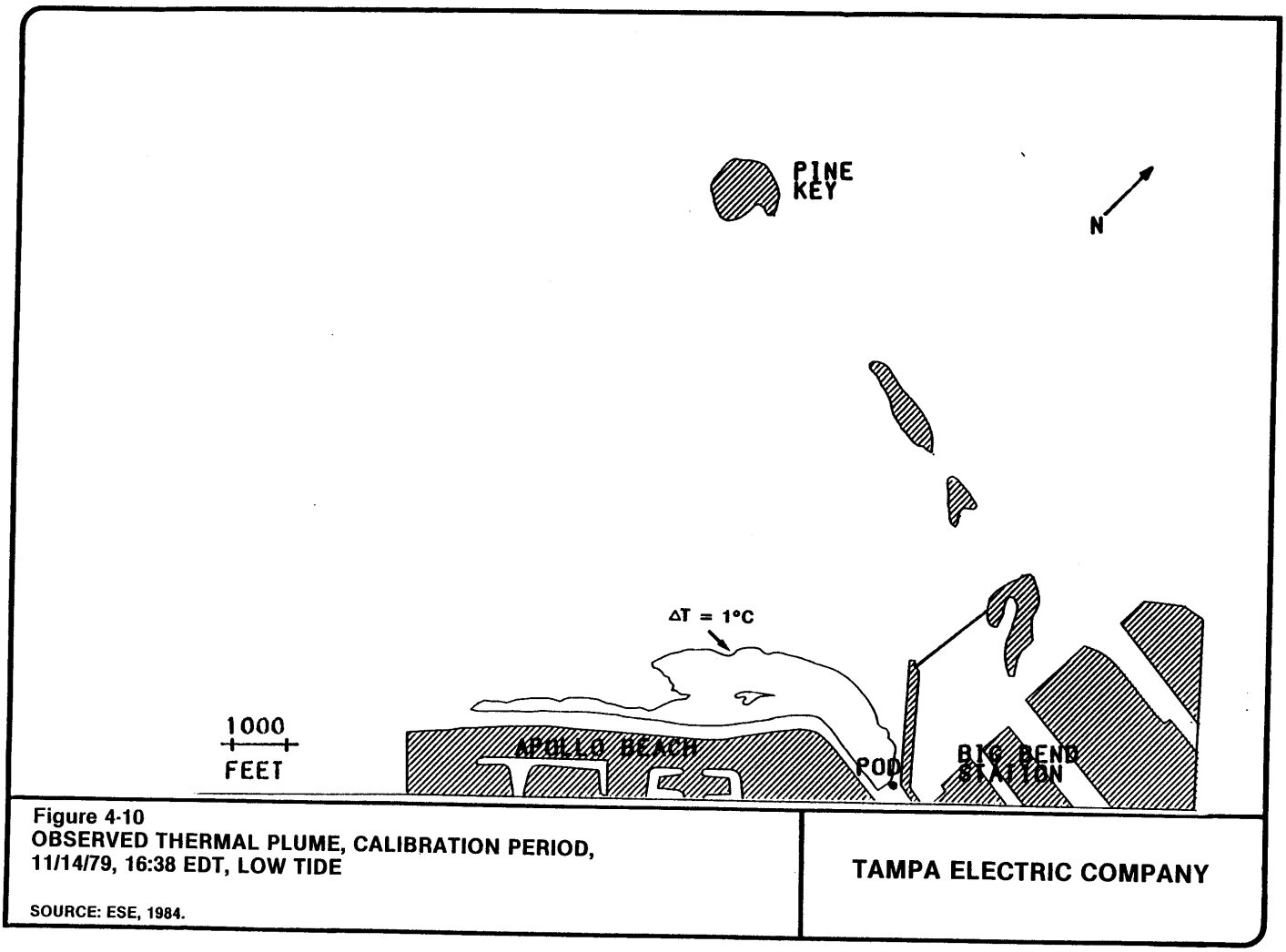

Figure 4-10
OBSERVED THERMAL PLUME, CALIBRATION PERIOD, 11/14/79, 16:38 EDT, LOW TIDE

SOURCE: ESE, 1984.

TAMPA ELECTRIC COMPANY

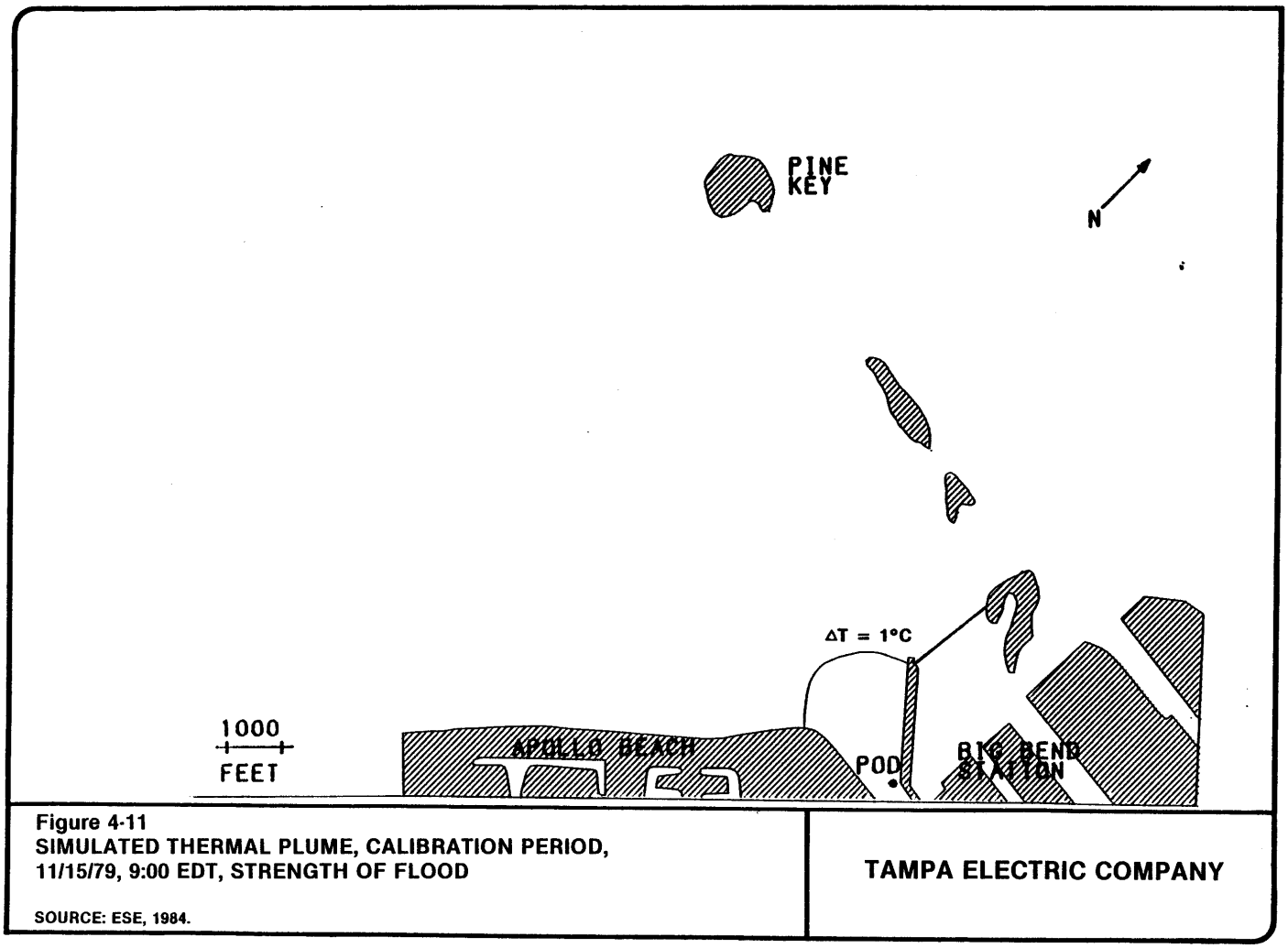

Figure 4-11
SIMULATED THERMAL PLUME, CALIBRATION PERIOD, 11/15/79, 9:00 EDT, STRENGTH OF FLOOD

SOURCE: ESE, 1984.

TAMPA ELECTRIC COMPANY

balanced, indigenous population of shellfish, fish, and wildlife in and on the body of water into which the discharge is to be made and such demonstration has not been rebutted. It is the intent of the Commission that to the extent practicable, proceedings under this provision should be conducted jointly with proceedings before the federal government under Section 316(a), Public Law 92-500.

Zones of mixing for blowdown discharges from recirculated cooling water systems, and for discharge from non-recirculated cooling water systems of existing sources, shall be established on the basis of the physical and biological characteristics of the RBW.

When a zone of mixing is established pursuant to this Subsection 17-3.05(1)(f), F.A.C., any otherwise applicable temperature limitations contained in Section 17-3.05(1), F.A.C., shall be met at its boundary; however, the Department may also establish maximum numerical temperature limits to be measured at the POD and to be used in lieu of the general temperature limits in Section 17-3.05(1), F.A.C., to determine compliance by the discharge with the established mixing zone and the temperature limits in Section 17-3.05(1), F.A.C.

The biological effects of the thermal discharge and the circulating water intake structure of the plant are discussed in the amendment. Studies designed to complement the 316 study, such as the Fine Mesh Screen Study and the 1979 Aquatic Ecology Study, are included in the appendices of the document. As part of the 316 Demonstration effort, the need for a thermal mixing zone has been established. Section 5.9 "Variances" discusses the thermal mixing zone.

Prior to conducting the studies, the applicant organized the "Biological Review Committee" (BRC), a volunteer group of regulatory agency representatives who reviewed scopes of work for the above studies and monitored study progress. Their involvement was solicited as reviewers of the studies, in particular, to provide guidance in the design of the studies and to suggest modifications to the study work plans. The U.S. Environmental Protection Agency, U.S. Fish and Wildlife Service, Florida Department of Environmental Regulations, and the Southwest Florida Water Management District, among others, are represented on the BRC.

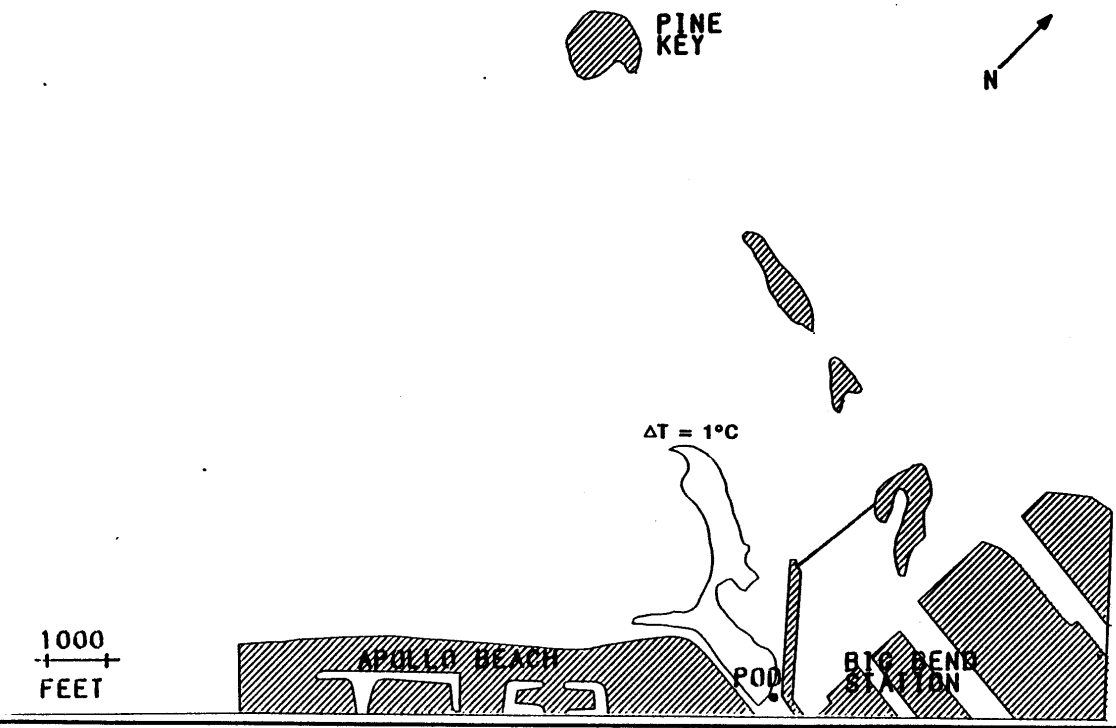

Figure 4-12
OBSERVED THERMAL PLUME, CALIBRATION PERIOD, 11/15/79, 8:51 EDT, STRENGTH OF FLOOD

SOURCE: ESE, 1984.

TAMPA ELECTRIC COMPANY

4.5 THERMAL VERIFICATION

The thermal verification was conducted by using the calibrated model to simulate November 17, 1979, when two aerial infrared photographs were available. The areas experiencing a surface temperature increase of 1°C over ambient temperature were determined by planimetry from the aerial photographs. The model simulation was begun at 3:00 a.m. Eastern Standard Time on November 16, 34 hours prior to the first time period compared with an observed plume. As discussed in Section 2.0, the thermal verification is independent of the calibration period, as more than 93 percent of the excess heat discharged to the bay during the calibration period had been lost to the atmosphere by the time the two verification photographs were taken.

The cool, dry weather pattern observed during the calibration period continued through the verification period. Thus, the same equations presented in Section 4.4 were also used to define the model heat exchange coefficient for the verification period. The heat exchange coefficients were adjusted to account for the fact that the calibration period indicated that the Edinger heat exchange coefficient must be increased by 9 percent to adequately reproduce observed plumes. The equation used to define the model heat exchange coefficient for the verification period is:

$$K_m = \frac{1.09\ K_e d_m}{(T_s - T_a)} \left[\frac{T_s - T_e}{d_m} - \frac{T_a - T_e}{H} \right] \qquad (4\text{-}10)$$

From the data sources previously described, the following parameter values were determined:

Wind Speed = 2.8 m/sec

T_a = 23.4°C

T_d = 7.5°C

T_p = 27.8°C

H = 2.3 m

S = 160 W/m^2

The average depth in the vicinity of the plume, H, is slightly larger in the verification period because the slightly larger plumes on November 17 extended into deeper water. From Equation 4-7, the average surface temperature of the plume is T_s = 26.1°C. From Edinger et al. (1974), K_e = 23 W/m^2/°C. From these two values, Equation 4-2 yields T_e = 14.5°C. Then, applying Equation 4-8, the model heat exchange coefficient, K_m = 54 W/m^2/°C, which again represents a 9-percent increase over the Edinger heat exchange coefficient, after accounting for the fact that ambient temperature was not at equilibrium.

Applying this heat exchange coefficient, the verification period was simulated using the hourly thermal loading data provided by TEC to define discharge conditions. Comparisons of predicted and observed thermal plumes during the verification period are shown in Figures 4-13 through 4-16.

The area of the first verification plume, as determined from aerial infrared survey, was 258 acres, while the model-simulated area was 351 acres. The second verification plume had an area of 447 acres, compared with a predicted area of 370 acres. The average size of the two verification plumes is reproduced accurately by the model, as the average predicted area is just 3 percent larger than the average observed area. The large difference between the first and second aerial infrared plumes is difficult to explain since there were only 2.4 hours between the two observations, and thermal loadings were not variable enough during this period to explain the significant increase in size of the second plume. Localized wind effects probably account for the increase in size as the second plume may have been blown further offshore. Further analysis of the differences between observed and predicted plumes is presented in the next section.

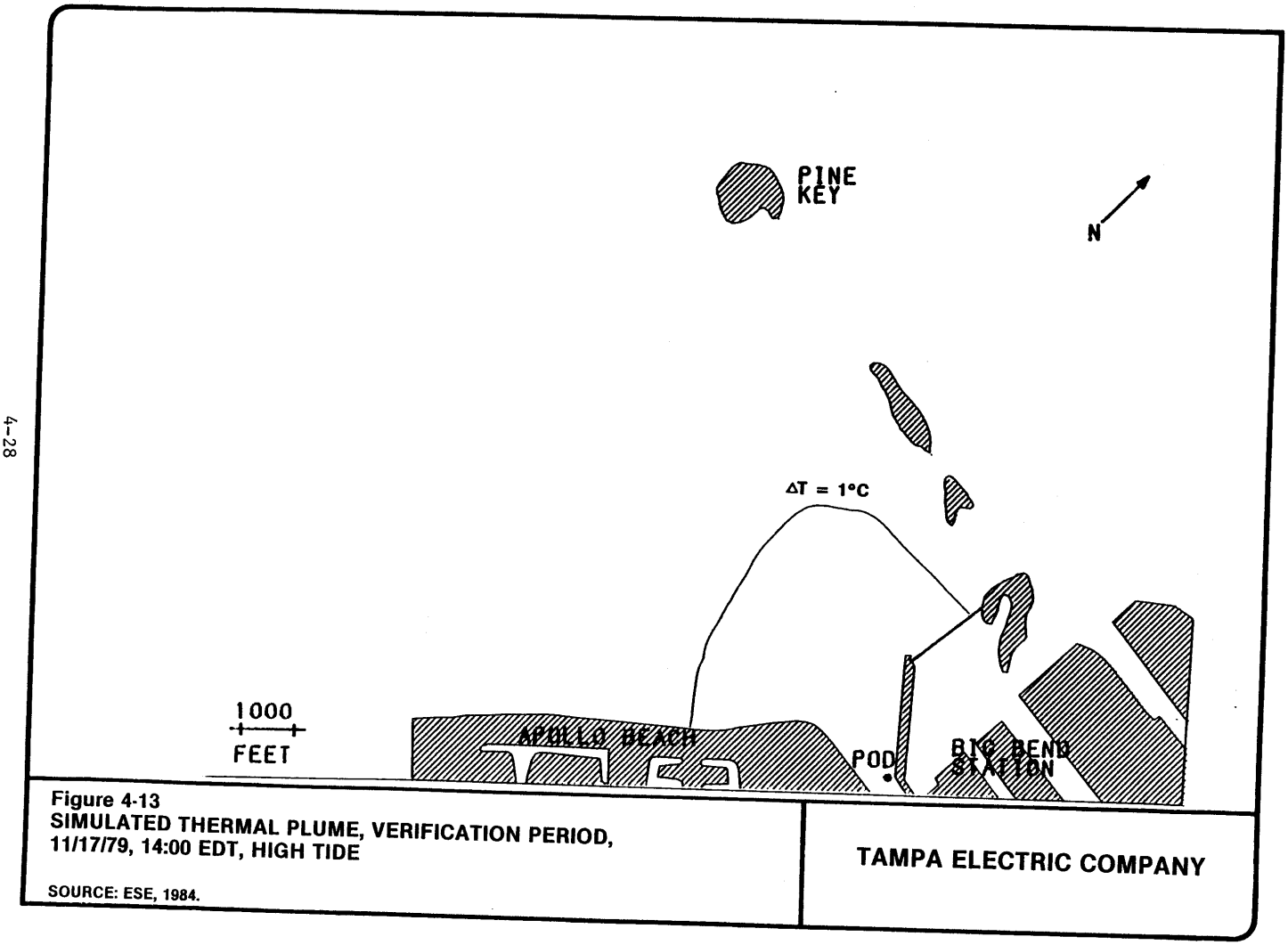

Figure 4-13
SIMULATED THERMAL PLUME, VERIFICATION PERIOD, 11/17/79, 14:00 EDT, HIGH TIDE

SOURCE: ESE, 1984.

TAMPA ELECTRIC COMPANY

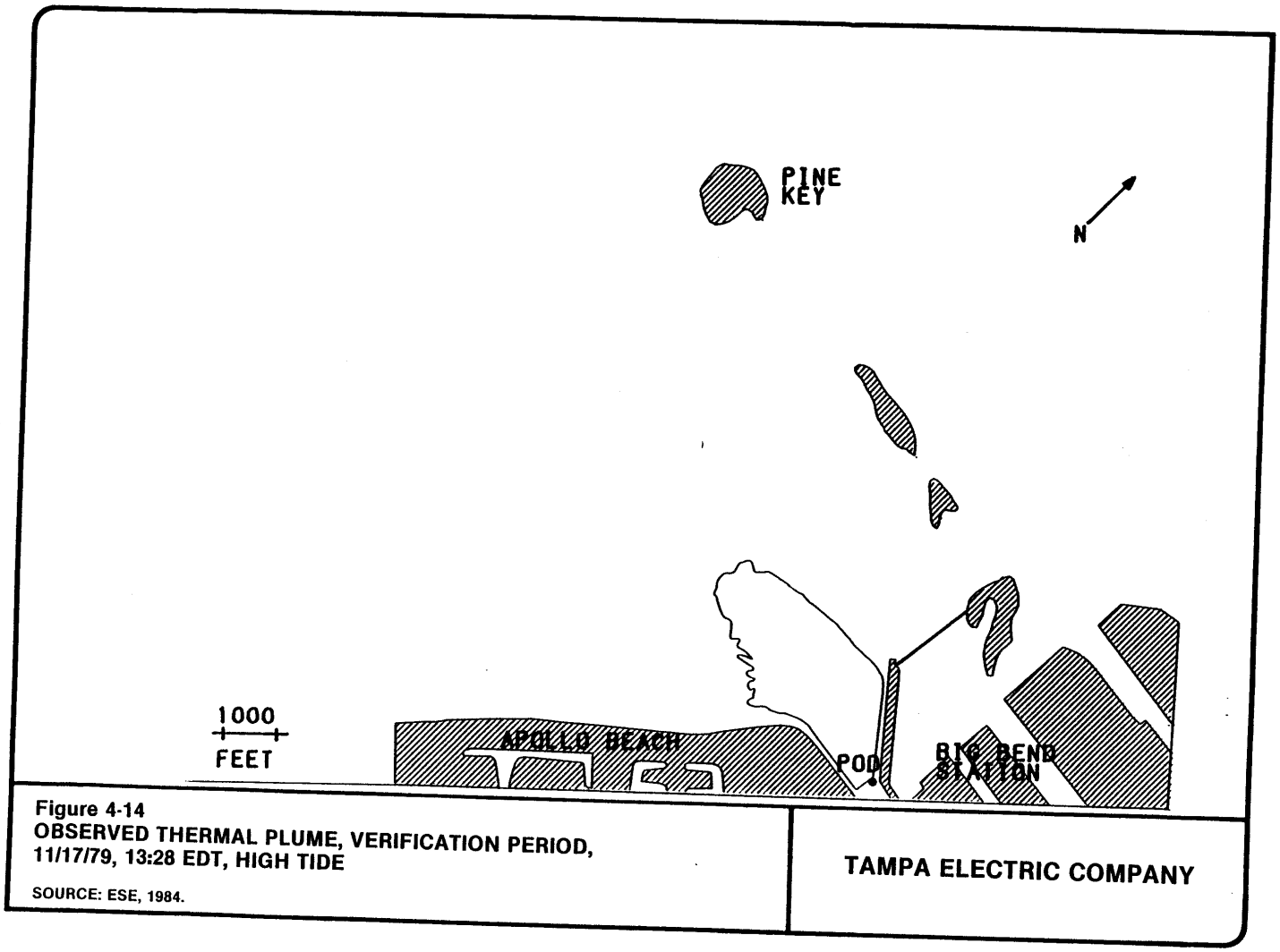

Figure 4-14
OBSERVED THERMAL PLUME, VERIFICATION PERIOD, 11/17/79, 13:28 EDT, HIGH TIDE

SOURCE: ESE, 1984.

TAMPA ELECTRIC COMPANY

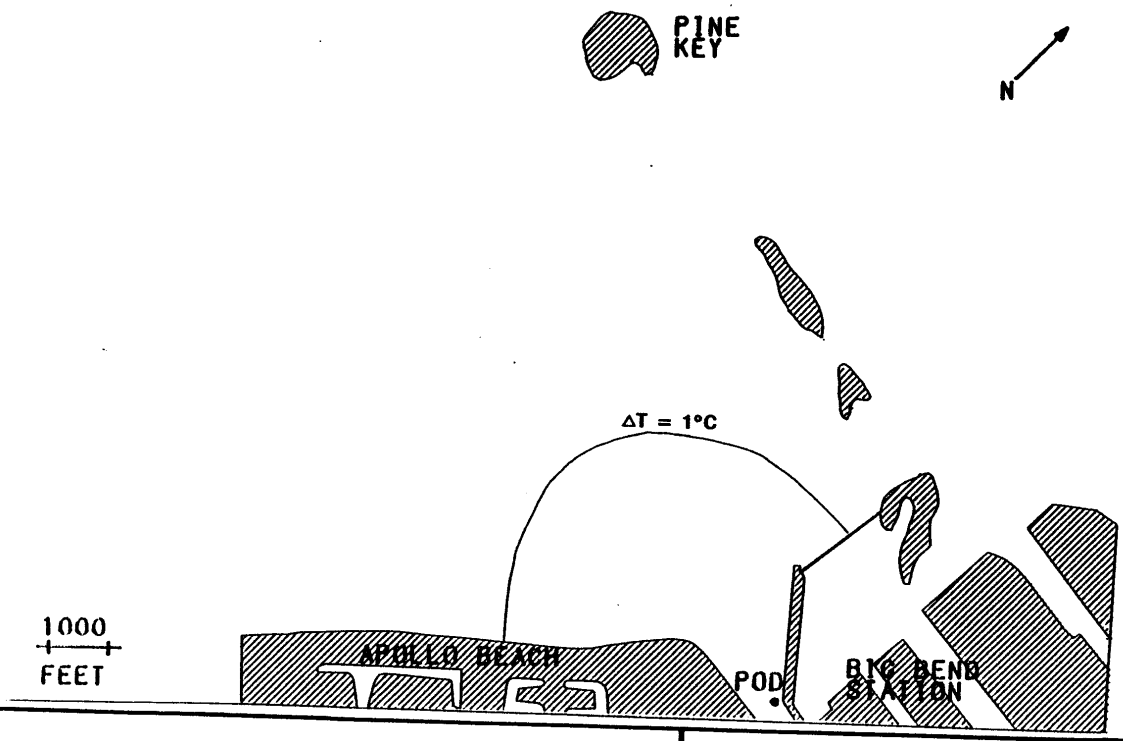

Figure 4-15
SIMULATED THERMAL PLUME, VERIFICATION PERIOD, 11/17/79, 16:00 EDT, STRENGTH OF EBB

SOURCE: ESE, 1984.

TAMPA ELECTRIC COMPANY

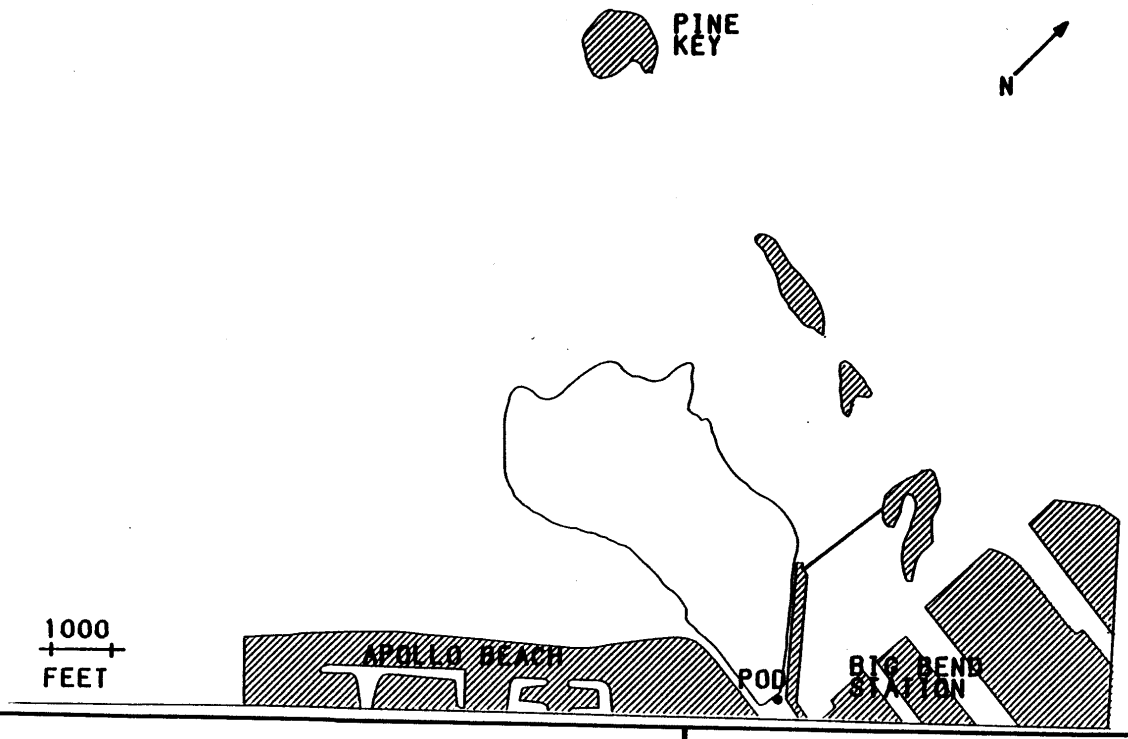

Figure 4-16
OBSERVED THERMAL PLUME, VERIFICATION PERIOD, 11/17/79, 15:53 EDT, STRENGTH OF EBB

SOURCE: ESE, 1984.

TAMPA ELECTRIC COMPANY

5.0 MODEL ACCURACY AND SENSITIVITY ANALYSIS

Model Accuracy--The calibration and verification process provides a good basis for characterizing the reliability of model results. In this section, statistical comparisons between observed data and model results will be summarized and interpreted.

During the verification of the hydraulic model, the standard deviation between predicted and observed water levels at Apollo Beach, Ballast Point, and Pendola Point was 3.7 cm. During this period, the average tidal range at these three stations was 0.46 m, so the typical error in individual water-level predictions was 8 percent of the range.

The difference between observed and predicted plume areas for the calibrated and verified model is summarized in Table 5-1. The average absolute error ranged from 22.5 percent in the calibration period to 27.5 percent in the verification period. The average absolute error over all four plumes was 25 percent. An alternate measure of error, the standard error, was calculated to be 26 percent. The average plume area as observed is 232 acres, while the average area of the corresponding modeled plumes is 240 acres, indicating a slight tendency for the model to overestimate the plume area by 3 to 5 percent. The correlation between predicted and observed plume area is 0.89. Based on four data points, this correlation is significant with 90 percent confidence. The regression equation expressing the relationship between modeled area and observed area is:

$$\text{Observed Area (acres)} = 0.97 \times \text{Modeled Area (acres)} - 0.6 \qquad (5\text{-}1)$$

The absolute difference, in acres, between predicted and observed plume size was correlated with the observed plume area. The correlation coefficient is 0.74, which is significant with 80 percent confidence. The

Table 5-1. Model Accuracy in Simulation of Thermal Mixing Zone Size (acres with $\Delta T > 1°C$)

	Observed Area	Simulated Area (Variance from Observed)
October 14, 16:38 EDT	124	155 (+25%)
October 15, 8:51 EDT	98	78 (-20%)
October 17, 13:28 EDT	258	356 (+38%)
October 17, 15:53 EDT	447	370 (-17%)

Source: ESE, 1984.

regression equation expressing the relationship between the absolute error and plume area is:

$$\text{Absolute Error (acres)} = 16.7 + 0.172 \text{ Area (acres)}$$

This relationship indicates that there is a small absolute error of about 17 acres regardless of plume size, but that if the area were larger (e.g., 2,000 acres), the prediction error should decrease to 17 to 18 percent.

This result was expected because the area of larger plumes will be governed by the heat exchange coefficient and tidal dynamics, both of which are described quite accurately by the CAFE-1/DISPER-1 models in this application. The size of the smaller plumes, which are the foundation of this calibration and verification process, are affected by the same phenomena, but are also significantly affected by the near-field dynamics of the discharge, which are not described in detail by CAFE-1/DISPER-1.

To summarize, the comparison of observed and predicted plumes indicates that the model tends to overpredict the plume area by 3 to 5 percent. Errors in reproducing individual plumes are random, and the typical error is 25 percent. The area of larger plumes, to be simulated under extreme conditions with four units, will be predicted more accurately than the smaller plumes of the calibration and verification periods, with typical random errors of about 18 percent expected.

Model Sensitivity--Sensitivity studies were planned only to the extent required to understand problems encountered in calibration, particularly if it was necessary to use parameter values which were not consistent with values determined by others from the technical literature. Such problems generally were not encountered, as discussed in Section 4.0. Parameter values required to achieve calibration are consistent with

guidance from the body of technical literature, generally within a few percent of an initial or "best" estimate derived from review of the literature, with the exception of the dispersion coefficient and the depth of mixing. Although the dispersion coefficient used is within the range of values reported by others (e.g., Murthy and Okubo, 1977), the range of values reported in the literature is broad, and it is clear that the model is sensitive to variations within this range. A meaningful sensitivity analysis could not be performed, however, because the model was unstable at the lower end of the range of literature values.

Thus, model sensitivity studies were only useful with respect to the depth of mixing. Although governed by the general requirement of Froude number similarity, the depth of mixing as defined in this study is a site-specific parameter which could not be defined by review of technical literature. Instead, it was defined from site-specific data. These data indicate that the depth of mixing is relatively constant over most of the plume and consistent from one data period to the next. These data do exhibit some variability, however, with a standard deviation of 0.35 m and a mean of 1.5. Thus, the actual depth of mixing may have been slightly greater or less than 1.5 m.

Sensitivity to the depth of mixing was investigated in the context of the worst case scenario under four unit operation, Scenario 2 (see Section 6.0). The best estimate for the depth of mixing under the discharge conditions of Scenario 2 is 1.8 m. The scenario was run for 250 hours, and the surface area enclosing the ambient +2°F isotherm was determined during the last flood phase. The model was rerun using a depth of mixing of 1.3 and 2.3 m, respectively. At d_m = 1.3 m, the mixing zone area was 4,379 acres; at d = 1.8 m, the area was 4,443 acres; while with d_m = 2.3 m, the area was 4,257 acres. The differences between the three simulated areas amount to less than 5 percent, while the depth of mixing was varied over 28 percent from the best estimate, indicating that the steady-state response of the model is relatively insensitive to

the depth of mixing. Reviewing the temporal response of the model, it was noted that DISPER-1 reached thermal equilibrium more rapidly with a lower depth of mixing. This implies that the response of the model to fluctuating thermal loading rate was a feature of the calibration and verification period, incorporation of this parameter was probably important to the success of the calibration. Under steady loads and a long simulation time, as used in the four unit scenario reported in Section 6.0, the results will be insensitive to the depth of mixing.

6.0 RESULTS

The calibrated and verified model was used to simulate the thermal mixing zone of the combined cooling water discharge from Big Bend Units 1 through 4, accounting for both the thermal and hydraulic loadings.

To validate that the mixing zone will conform to specific limits under future conditions which are unpredictable, the range of scenarios which could be simulated is infinite. As a practical matter, it is necessary to capsulize the range of possible conditions in a finite number of scenarios. The most important variables that can affect mixing zone size are season, tidal fluctuations, winds, and thermal load. The objective in scenario selection was to define conditions which may reasonably be expected to occur, and to identify combinations of those conditions which result in the greatest impact. The 10 scenarios selected for this study are specified in Table 6-1.

Two plant operational scenarios were simulated: 100-percent load and the normal operating load factor of 65 percent. These operational scenarios were simulated under both winter and summer conditions. The largest absolute temperatures are experienced in the summer, while the largest incremental temperatures occur in winter. Data supplied by the National Climatic Center, which characterize the frequency of wind speed and direction on a seasonal basis, were reviewed. The following winds are representative of commonly encountered winter winds which will reproduce the expected range of circulation patterns and mixing zones in Tampa Bay: east-northeast at 8.5 knots (kts), north at 8.5 kts, and south at 8.5 kts. During summer, the clearly predominant wind direction is from the east, and 8.5 kts is a typical speed. Westerly winds were not included in this set because they are not common during either the winter or summer. In addition to normal tidal conditions, spring and neap tides were also simulated, resulting in 10 scenarios. The normal tide was diurnal with a range of 2.3 ft at St. Petersburg. The spring

Table 6-1. Scenarios for Simulation of Four Unit Mixing Zone

Scenario	Season	Power Plant Loading (Percent Capacity)	Temperature Rise at POD (°F)	Wind	Tidal Range	Ambient Temp. (°F)	Heat Exchange Coefficient ($W/m^2/°C$)	Depth of Mixing (m)
1	Winter	100	16.8	Calm	Normal	53.6	21	2.2
2	Summer	100	16.8	Calm	Normal	86.0	32	1.8
3	Winter	65	10.9	Calm	Normal	53.6	20	2.6
4	Summer	65	10.9	Calm	Normal	86.0	31	2.2
5	Winter	100	16.8	ENE 8.5 kts	Normal	53.6	30	2.2
6	Winter	100	16.8	N 8.5 kts	Normal	53.6	30	2.2
7	Winter	100	16.8	S 8.5 kts	Normal	53.6	30	2.2
8	Summer	100	16.8	E 8.5 kts	Normal	86.0	48	1.8
9	Winter	100	16.8	Calm	Spring	53.6	21	2.2
10	Winter	100	16.8	Calm	Neap	53.6	21	2.2

Source: ESE, 1984.

tide simulated in Scenario 9 was diurnal with a range of 2.8 ft at St. Petersburg. The neap tide simulated in Scenario 10 was semidiurnal with a range of 1.4 ft.

Scenarios 1 through 4 characterize calm conditions when surface heat exchange is minimized, and the selection of seasonal and load conditions bracket expected ranges of thermal load and dissipation. Scenarios 1 and 2 are the basic winter and summer extreme scenarios. Scenarios 3 and 4 provide a more representative scenario under typical plant operating conditions, but still maintain calm wind conditions, which are atypical and conservative. Scenarios 5 through 7 account for commonly encountered wind patterns emphasizing winter conditions at 100-percent load, which leads to maximum thermal plume size, while the range of wind directions brackets the plume boundaries in various directions. Scenario 8 represents the maximum absolute temperature situation under typical summer winds. Scenarios 9 and 10 bracket the effects of extreme tides under conditions of maximum plume size.

The ambient temperatures for winter and summer conditions are those reported in the 316 Demonstration Report (TECO, 1980). Heat exchange coefficients were determined by reference to Figure 2.4.2 of Edinger et al. (1974). The values determined from that source were multiplied by 1.09 in accordance with the model calibration results.

The depth of mixing varies with temperature and discharge flow rate in accordance with Equation 3-3, upon the condition that the critical Froude number at the discharge is invariant.

The model was used to simulate each scenario for a period of 250 hours. Preliminary calculations indicated that this period was adequate to reach thermal equilibrium in the bay. Furthermore, it is unrealistic to anticipate that the plant would operate at 100 percent of capacity continuously for such an extended period. Results were reviewed after

simulation, and it was determined that the thermal mixing zone area was indeed close to equilibrium for all scenarios after 250 hours.

During the last tidal cycle of each simulation, the thermal mixing zone temperature was plotted at low water slack, strength of flood, high water slack, and strength of ebb, and the critical isotherm was contoured. The critical isotherm is 2°F for the summer scenarios and 4°F for the winter scenarios in accordance with FAC 17-3.05. The area within the critical contour was determined by planimetry. The resulting thermal mixing zone areas are presented in Table 6-2. The largest instantaneous area is 4,539 acres and occurs at strength of ebb for Scenario 2 (Summer, 100 percent of capacity, calm). The largest winter mixing zone is 2,653 acres, occurring at high slack for Scenario 1 (Winter, 100 percent of capacity, calm). The thermal mixing zone tends to be smaller in winter than in summer because of the more stringent excess temperature standard during the summer months.

Typical Conditions--Scenarios 3 and 4 represent typical power plant operating conditions (65-percent capacity), combined with calm winds for winter and summer, respectively. Isotherms for these scenarios at low water slack and high water slack are shown in Figures 6-1 through 6-4. The largest instantaneous plume is 2,793 acres at high water slack under summer conditions. The tidally averaged plume size is 2,641 acres during the summer (Scenario 4), but only 1,297 acres during winter.

Scenario 8 also represents a condition which can be considered typical for the summer season when power demands are high. Scenario 8 represents the maximum power plant loading (100-percent capacity) combined with the typical seasonal wind conditions (east at 8.5 kts). The largest plume under this scenario is 2,860 acres on strength of flood. The tidal averaged plume size is 2,730 acres. Figures 6-5 and 6-6 show the isotherms for this scenario at low and high water slack, respectively.

Table 6-2. Thermal Mixing Zone Areas by Scenarios

Scenario	Area of Thermal Mixing Zone (Acres)				
	Low Water Slack	Strength of Flood	High Water Slack	Strength of Ebb	Average
1	2,425	2,417	2,653	2,434	2,482
2*	4,489	4,443	4,224	4,539	4,424
3	1,249	1,313	1,316	1,310	1,297
4*	2,610	2,563	2,793	2,597	2,641
5	1,420	1,666	1,659	1,541	1,572
6	1,733	1,745	1,658	1,628	1,691
7	1,540	1,583	1,586	1,534	1,561
8*	2,823	2,860	2,741	2,496	2,730
9	2,531	2,336	2,435	2,316	2,405
10	1,791	1,832	1,848	1,843	1,829

* Plume size defined by the 2°F isotherm (summer criteria). All other scenarios plume size is defined by 4°F isotherm.

Source: ESE, 1984.

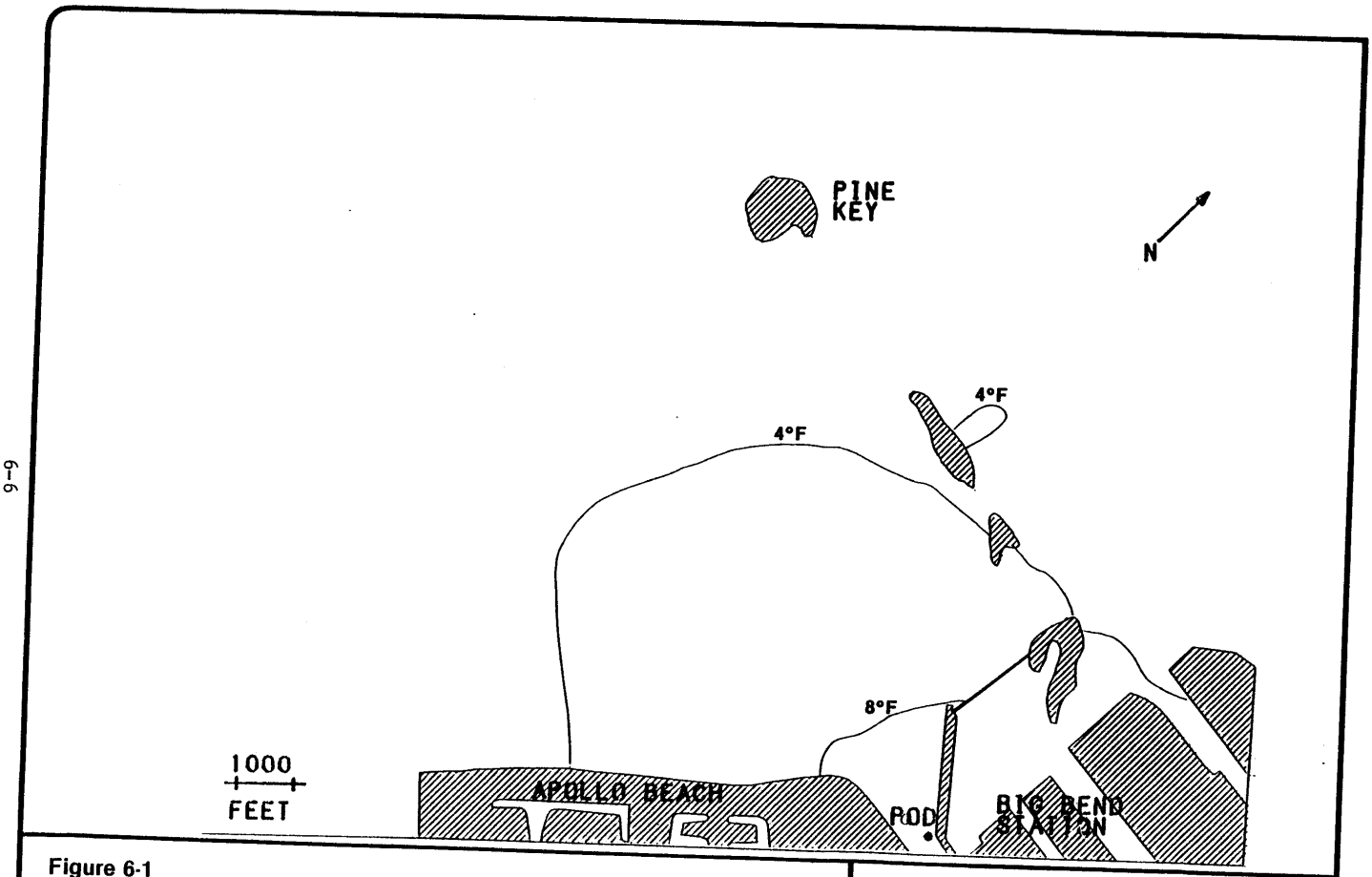

Figure 6-1
SCENARIO 3: LOW SLACK
AREA = 1,249 ACRES
SOURCE: ESE, 1984.

TAMPA ELECTRIC COMPANY

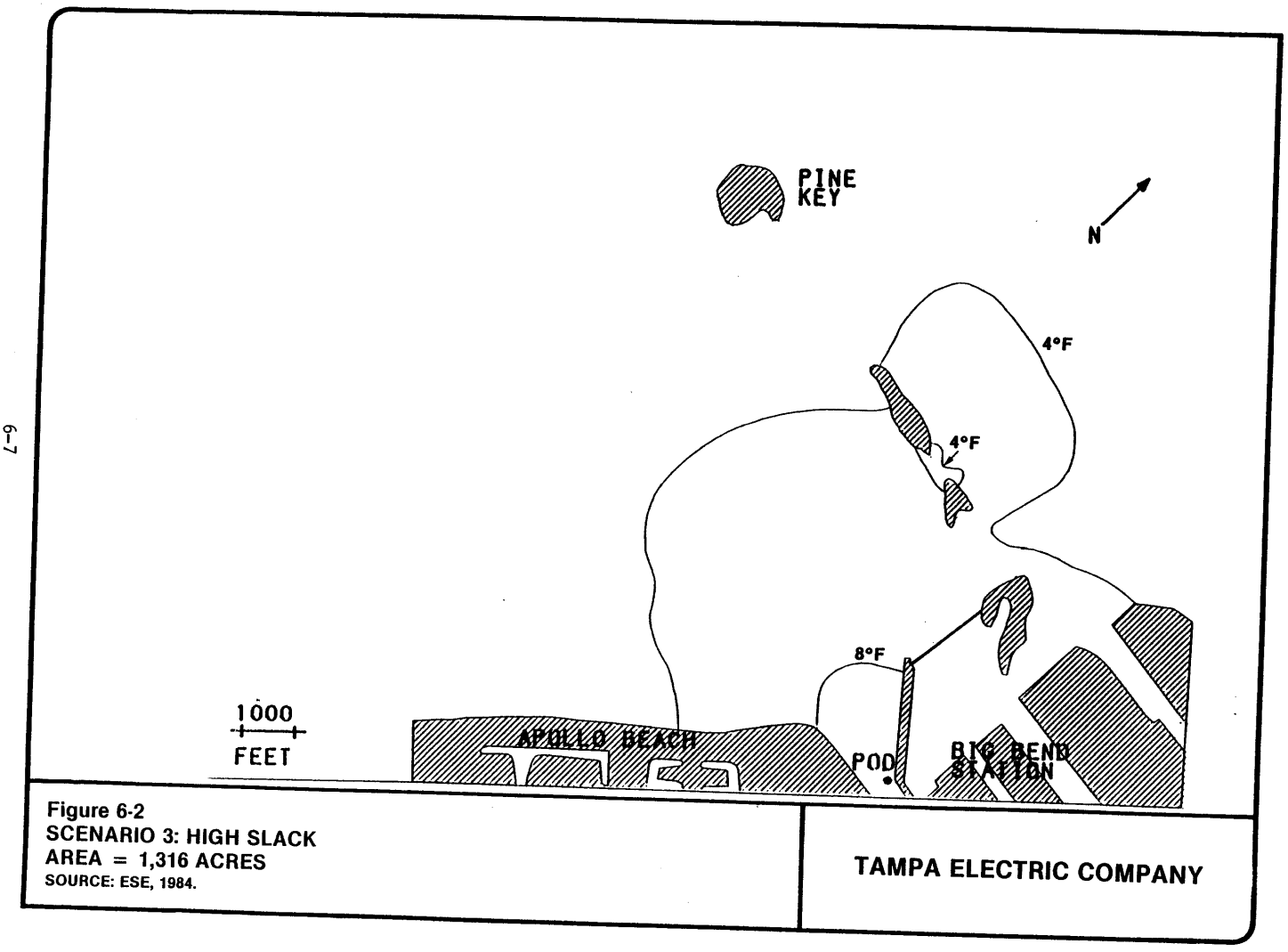

Figure 6-2
SCENARIO 3: HIGH SLACK
AREA = 1,316 ACRES
SOURCE: ESE, 1984.

TAMPA ELECTRIC COMPANY

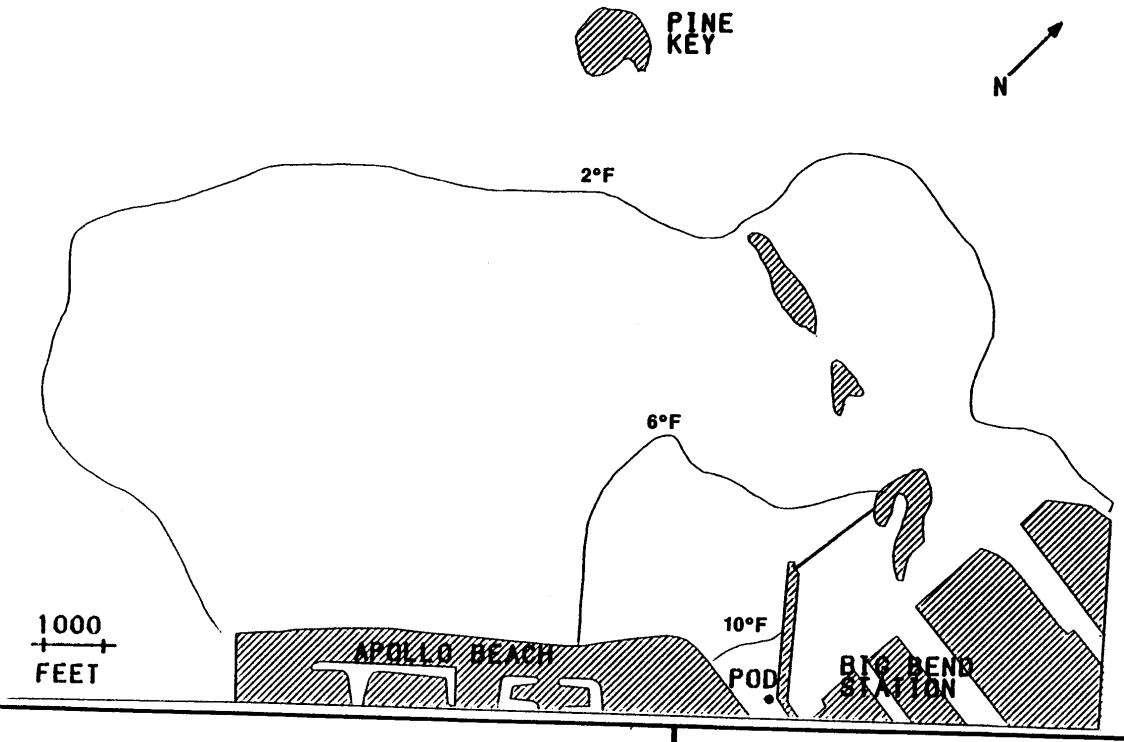

Figure 6-3
SCENARIO 4: LOW SLACK
AREA = 2,610 ACRES
SOURCE: ESE, 1984.

TAMPA ELECTRIC COMPANY

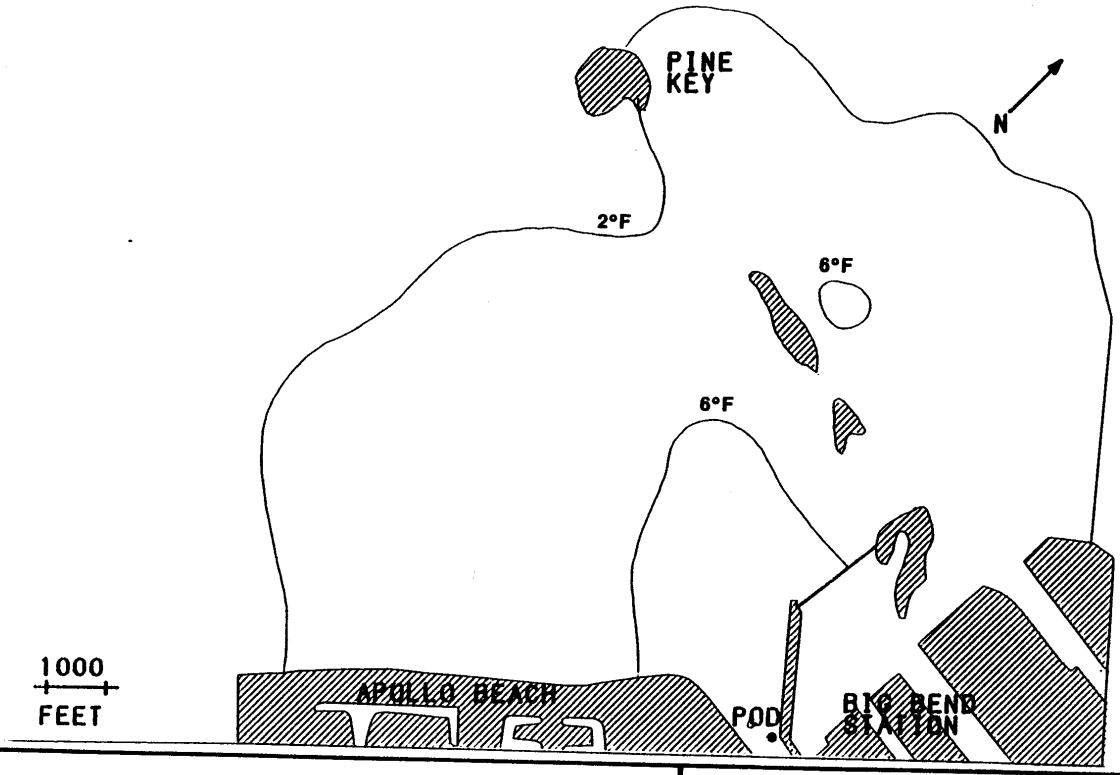

Figure 6-4
SCENARIO 4: HIGH SLACK
AREA = 2,793 ACRES
SOURCE: ESE, 1984.

TAMPA ELECTRIC COMPANY

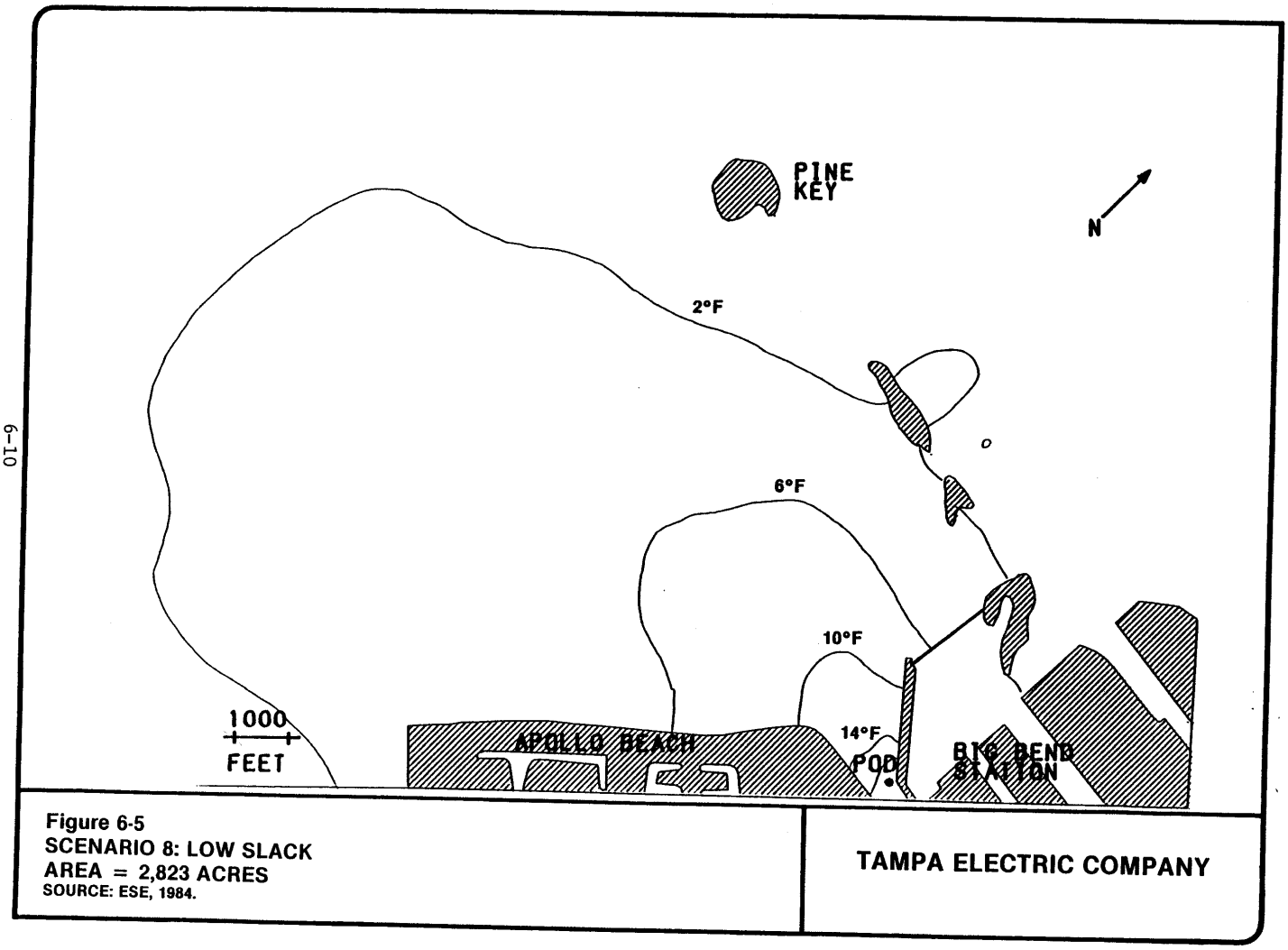

Figure 6-5
SCENARIO 8: LOW SLACK
AREA = 2,823 ACRES
SOURCE: ESE, 1984.

TAMPA ELECTRIC COMPANY

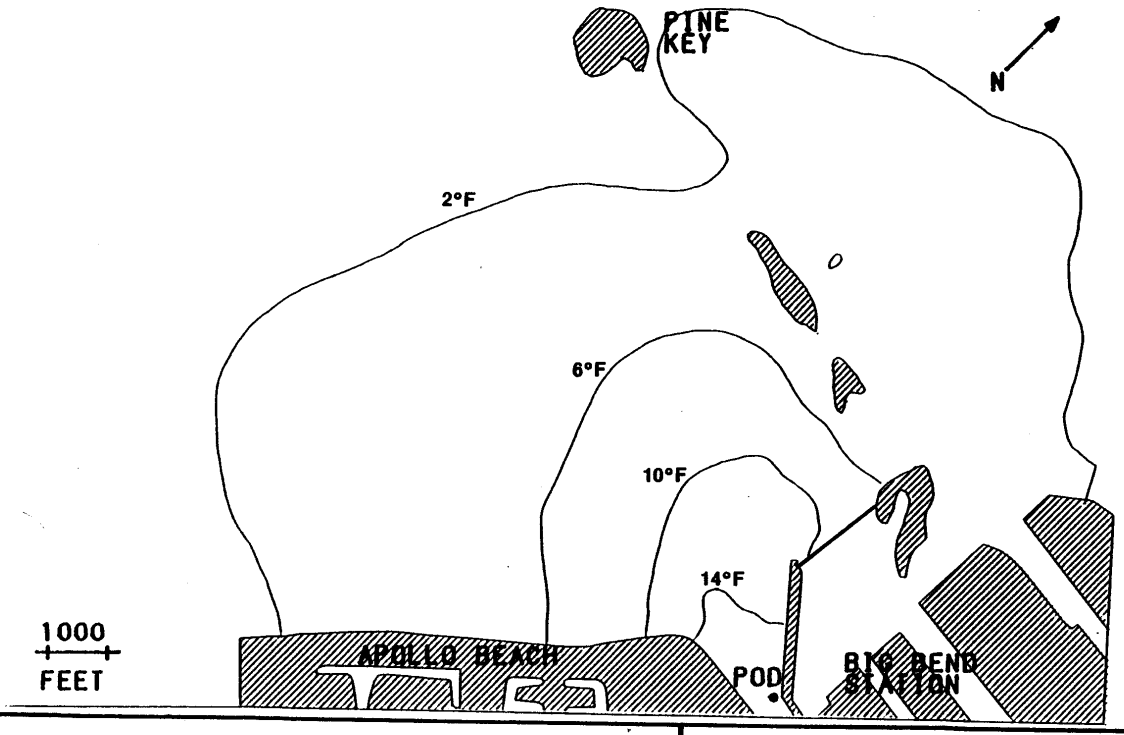

Figure 6-6
SCENARIO 8: HIGH SLACK
AREA = 2,741 ACRES
SOURCE: ESE, 1984.

TAMPA ELECTRIC COMPANY

Based on Scenarios 3, 4, and 8, the typical thermal plume created by the operation of Units 1 through 4 is expected to be between 1,200 and 2,900 acres.

Extreme Conditions--Extreme conditions for the winter and summer seasons are represented by Scenarios 1 and 2, respectively. These scenarios combine conditions of maximum thermal load and the minimum heat dissipation. The largest instantaneous plume size is 4,539 acres on strength of ebb during the summer. During the winter, the maximum plume size is 2,653 acres. Figures 6-7 through 6-10 show the plume isotherms for Scenario 1 at low water slack, strength of flood, high water slack, and strength of ebb. Figures 6-11 through 6-14 show the isotherms for the same four tidal phases for Scenario 2.

Effects of Wind--The effect of wind on the size and location of the thermal plume can be assessed by comparing Scenarios 1, 5, 6, and 7. All of these scenarios are for winter conditions, at 100-percent power plant load capacity, with normal tides. The only difference in these scenarios is the wind direction and speed. Figures 6-15 and 6-16 show the critical contours for these scenarios at low and high water slack, respectively. The most significant effect of wind is to reduce the overall size of the plume by increasing surface heat exchange. This effect is illustrated in Figures 6-15 and 6-16 by the fact that the critical contour for Scenario 1 (calm) encloses the contours of all the other scenarios.

As shown in Table 6-2, the average plume size for Scenarios 5, 6, and 7 is only 65 percent of the Scenario 1 plume. A secondary effect of wind is a change in the location of the critical contour. As expected, winds from the south move the plume north, while northerly winds move the plume south.

Effects of Tide--Tidal range and period had an effect on the mixing zone area. This is illustrated by comparison of Scenarios 1, 9, and 10. As

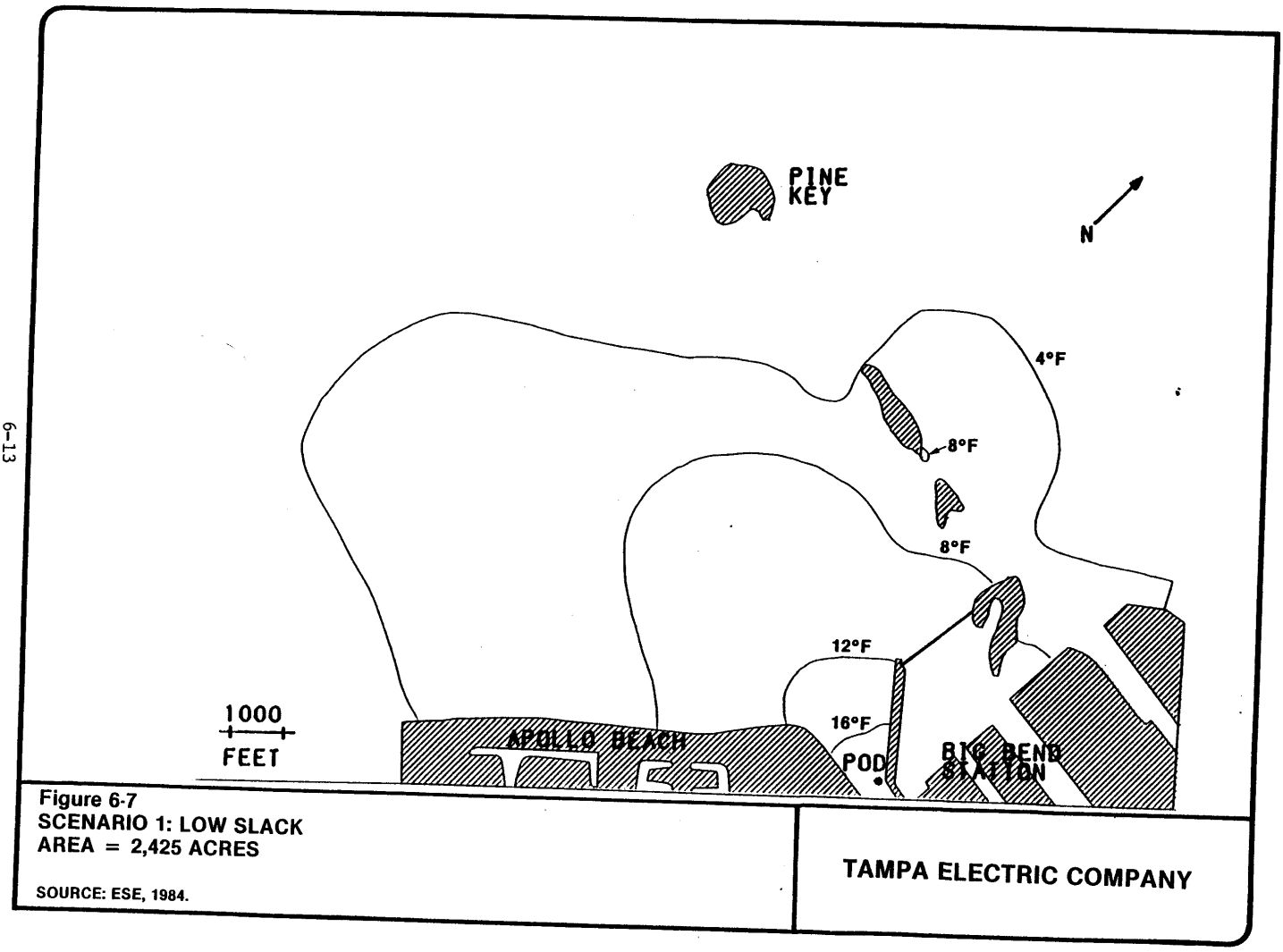

Figure 6-7
SCENARIO 1: LOW SLACK
AREA = 2,425 ACRES

SOURCE: ESE, 1984.

TAMPA ELECTRIC COMPANY

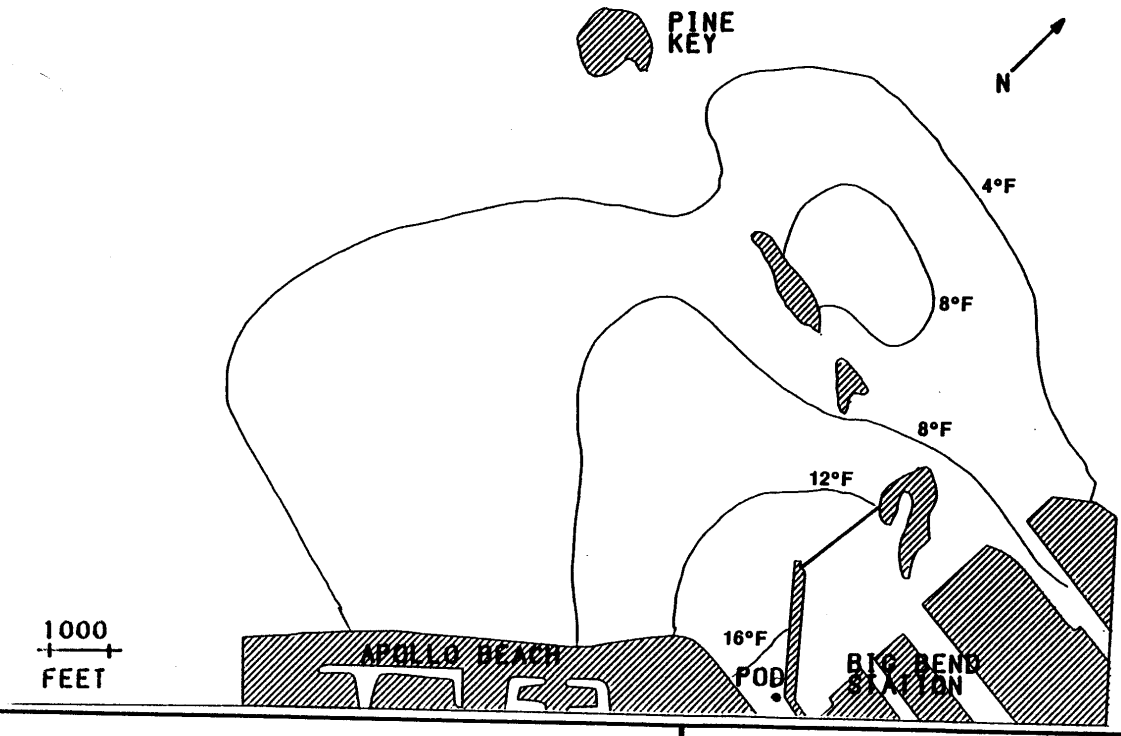

Figure 6-8
SCENARIO 1: STRENGTH OF FLOOD
AREA = 2,417 ACRES

SOURCE: ESE, 1984.

TAMPA ELECTRIC COMPANY

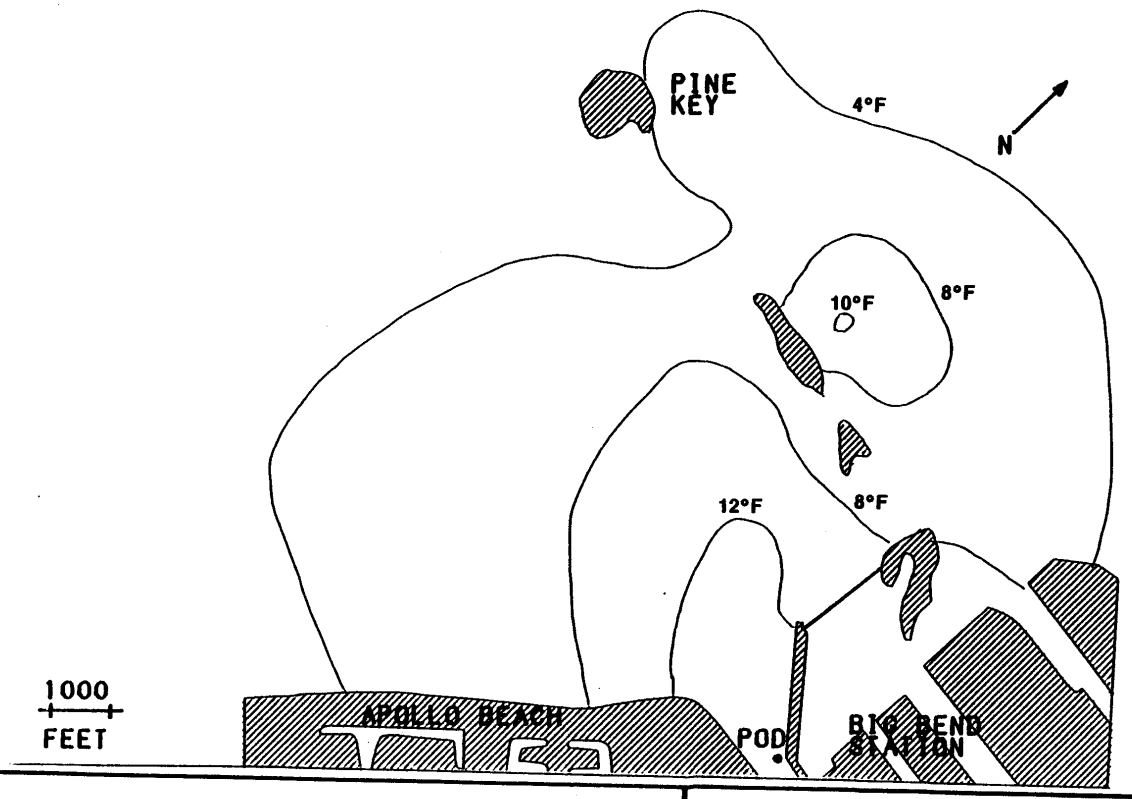

Figure 6-9
SCENARIO 1: HIGH SLACK
AREA = 2,666 ACRES

SOURCE: ESE, 1984.

TAMPA ELECTRIC COMPANY

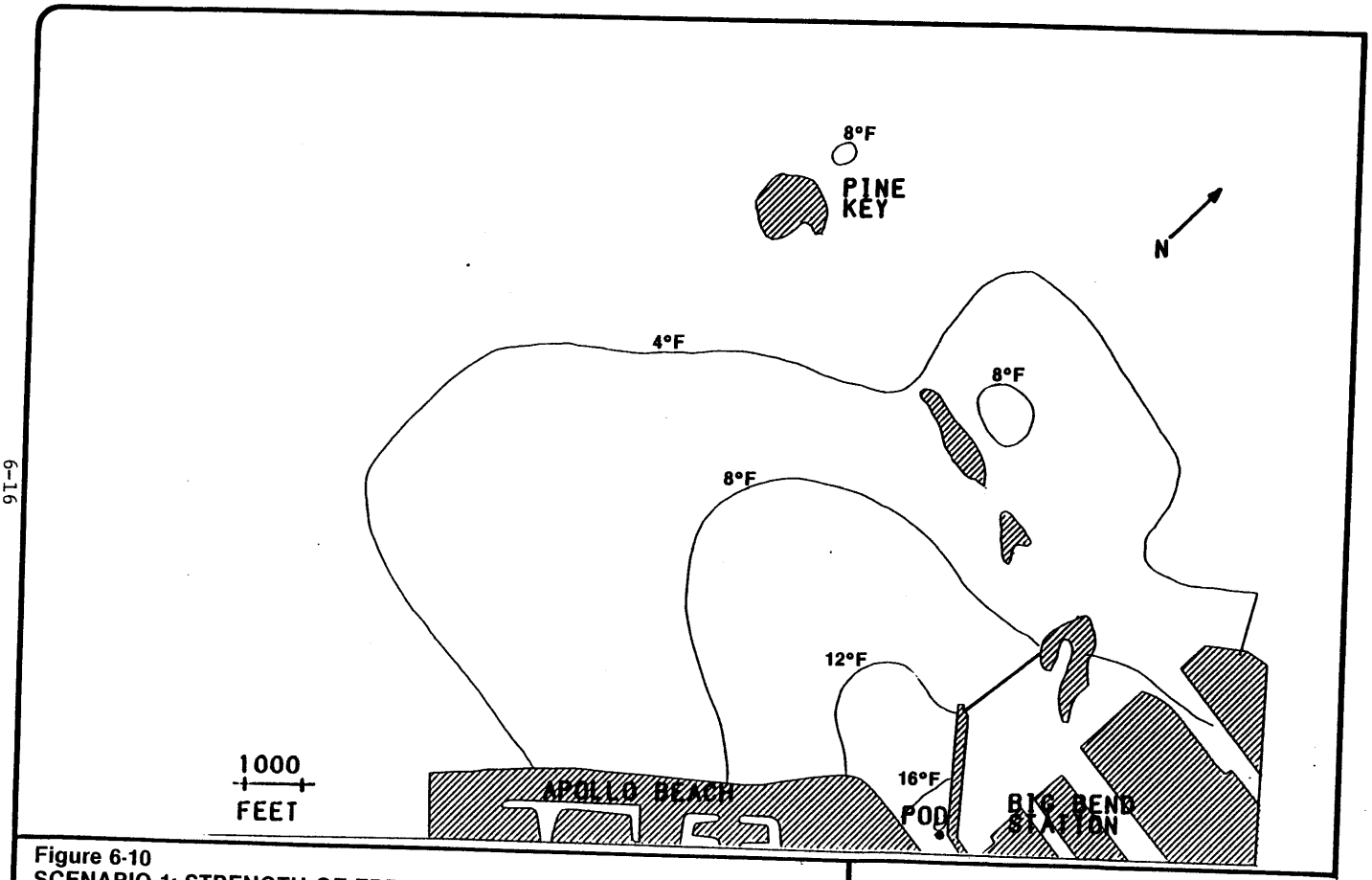

Figure 6-10
SCENARIO 1: STRENGTH OF EBB
AREA = 2,486 ACRES

SOURCE: ESE, 1984.

TAMPA ELECTRIC COMPANY

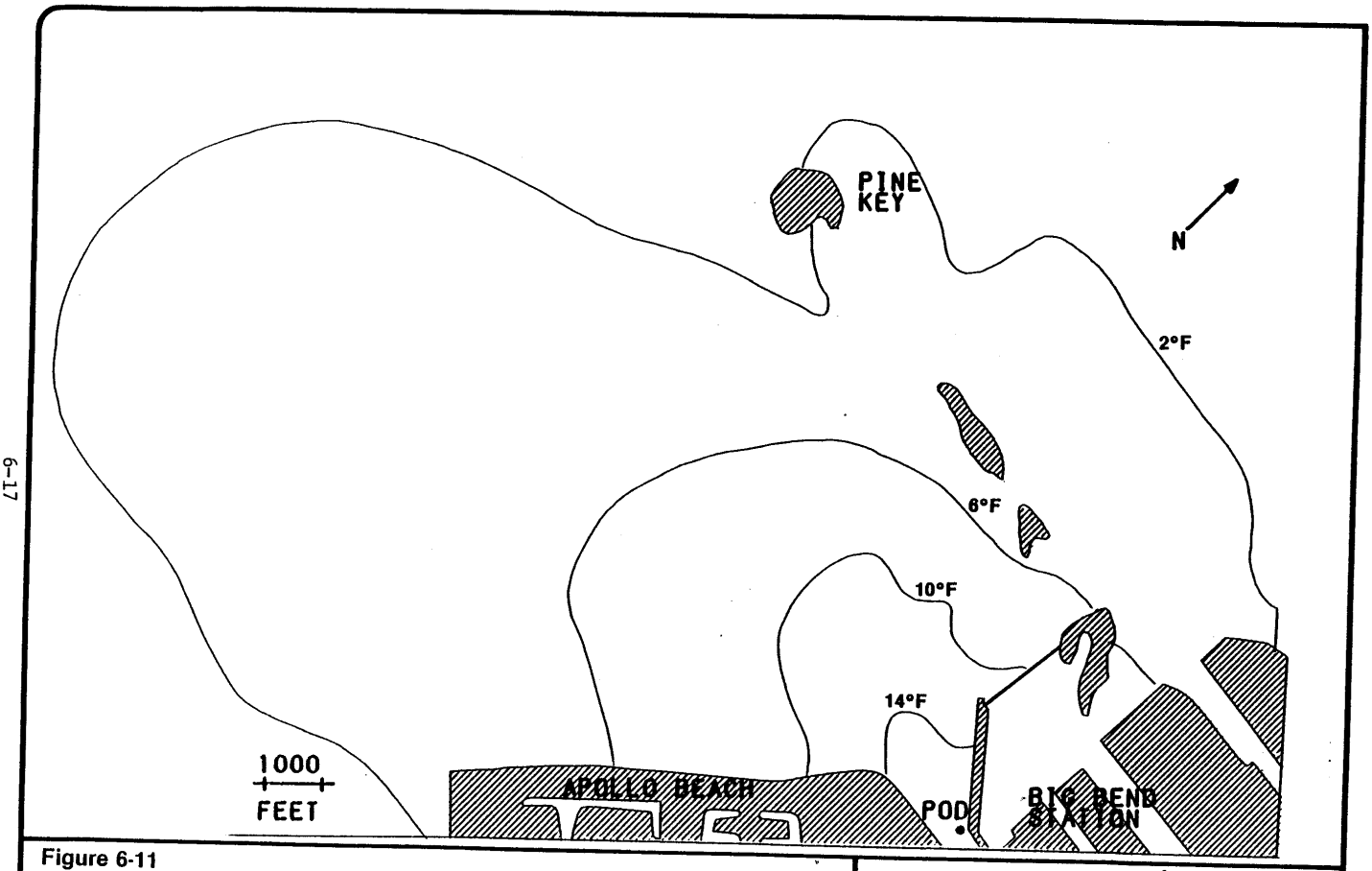

Figure 6-11
SCENARIO 2: LOW SLACK
AREA = 4,489 ACRES

SOURCE: ESE, 1984.

TAMPA ELECTRIC COMPANY

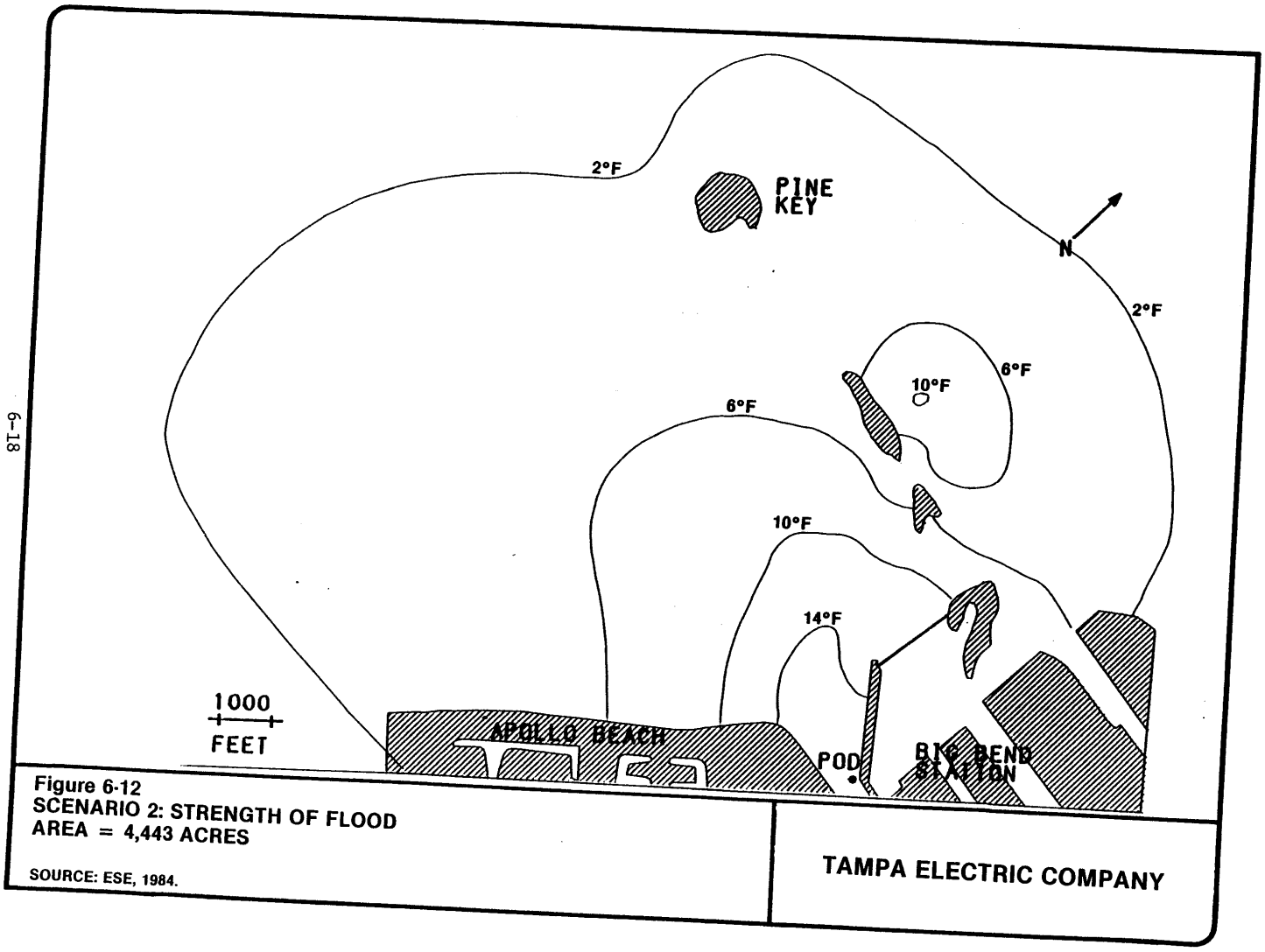

Figure 6-12
SCENARIO 2: STRENGTH OF FLOOD
AREA = 4,443 ACRES

SOURCE: ESE, 1984.

TAMPA ELECTRIC COMPANY

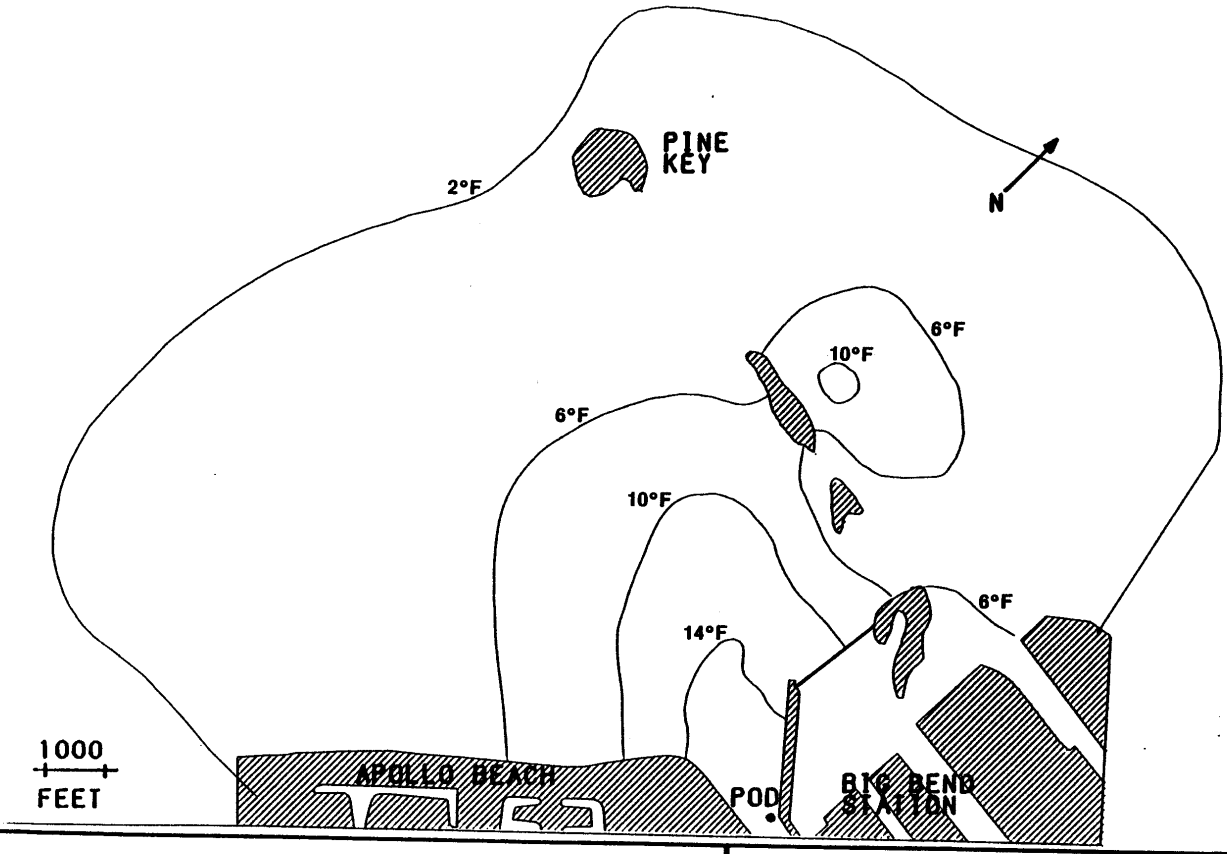

Figure 6-13
SCENARIO 2: HIGH SLACK
AREA = 4,224 ACRES

SOURCE: ESE, 1984.

TAMPA ELECTRIC COMPANY

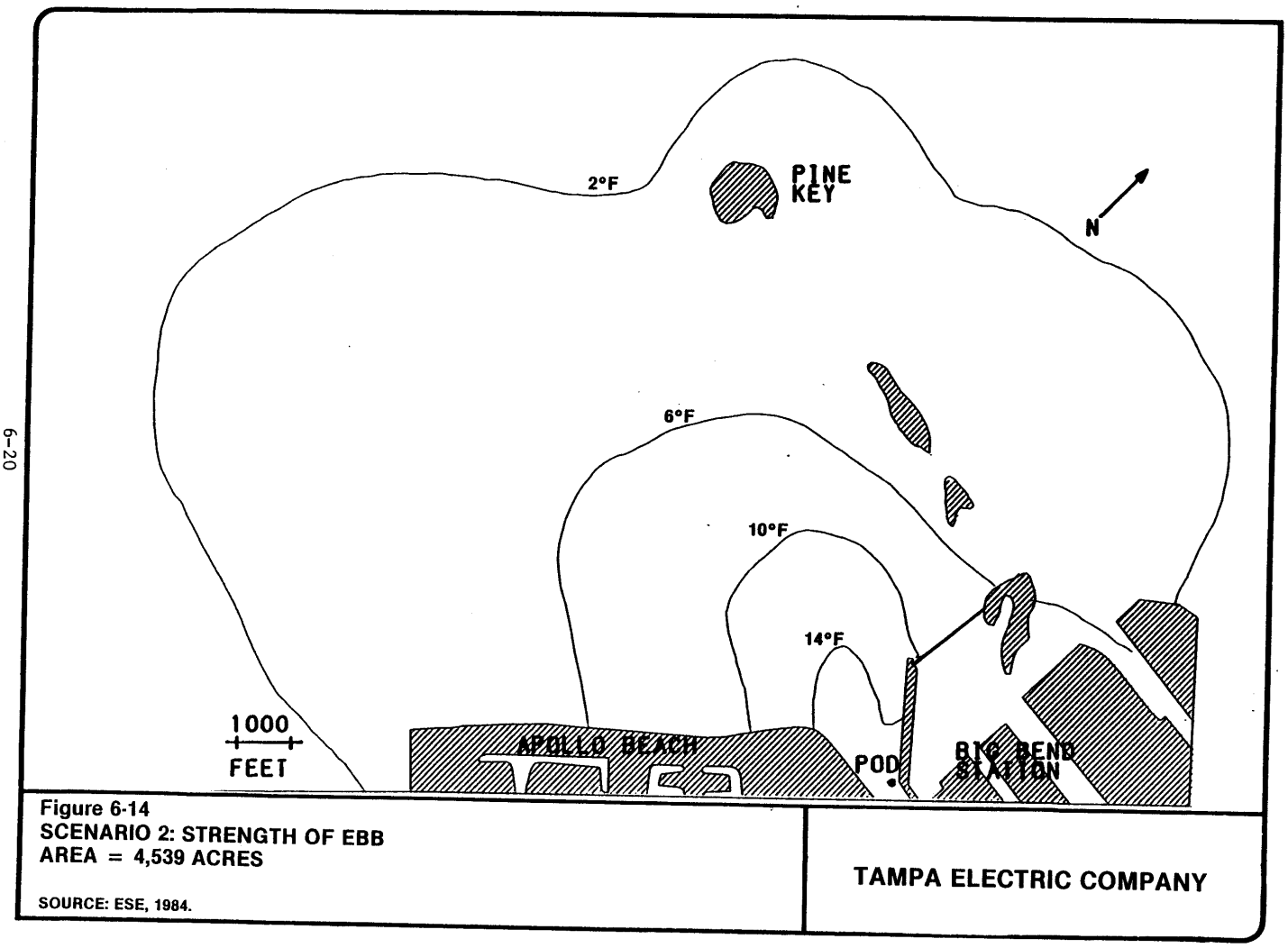

Figure 6-14
SCENARIO 2: STRENGTH OF EBB
AREA = 4,539 ACRES

SOURCE: ESE, 1984.

TAMPA ELECTRIC COMPANY

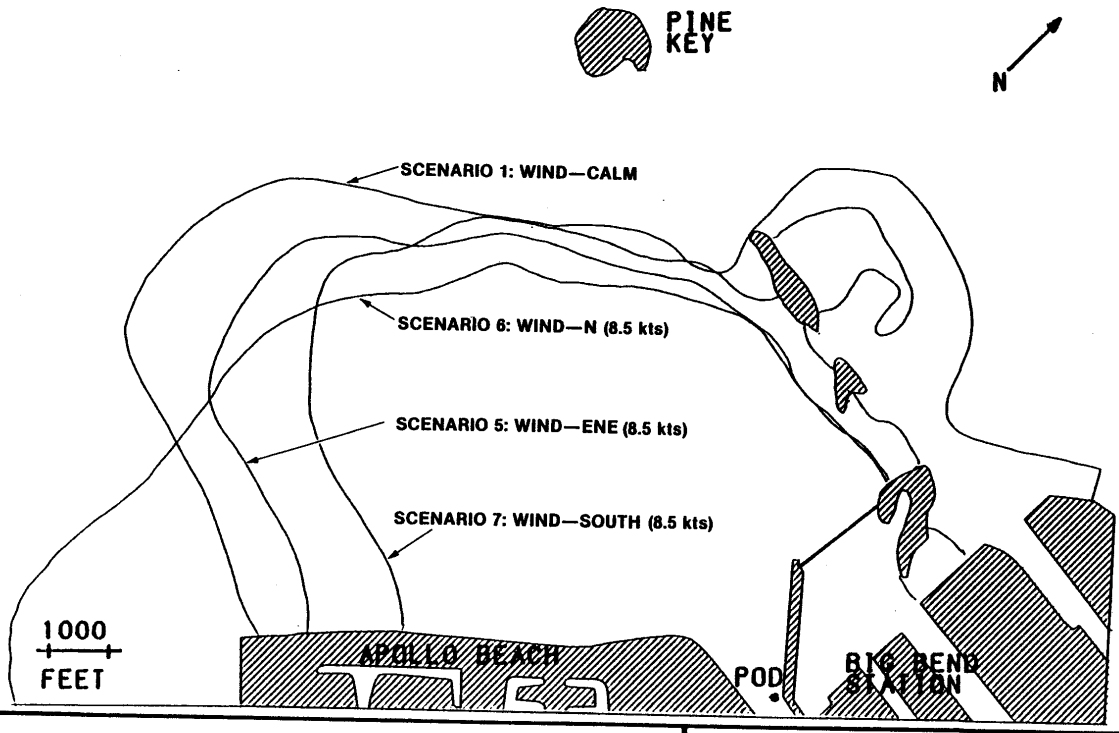

Figure 6-15
EFFECT OF WIND AT LOW SLACK

SOURCE: ESE, 1984.

TAMPA ELECTRIC COMPANY

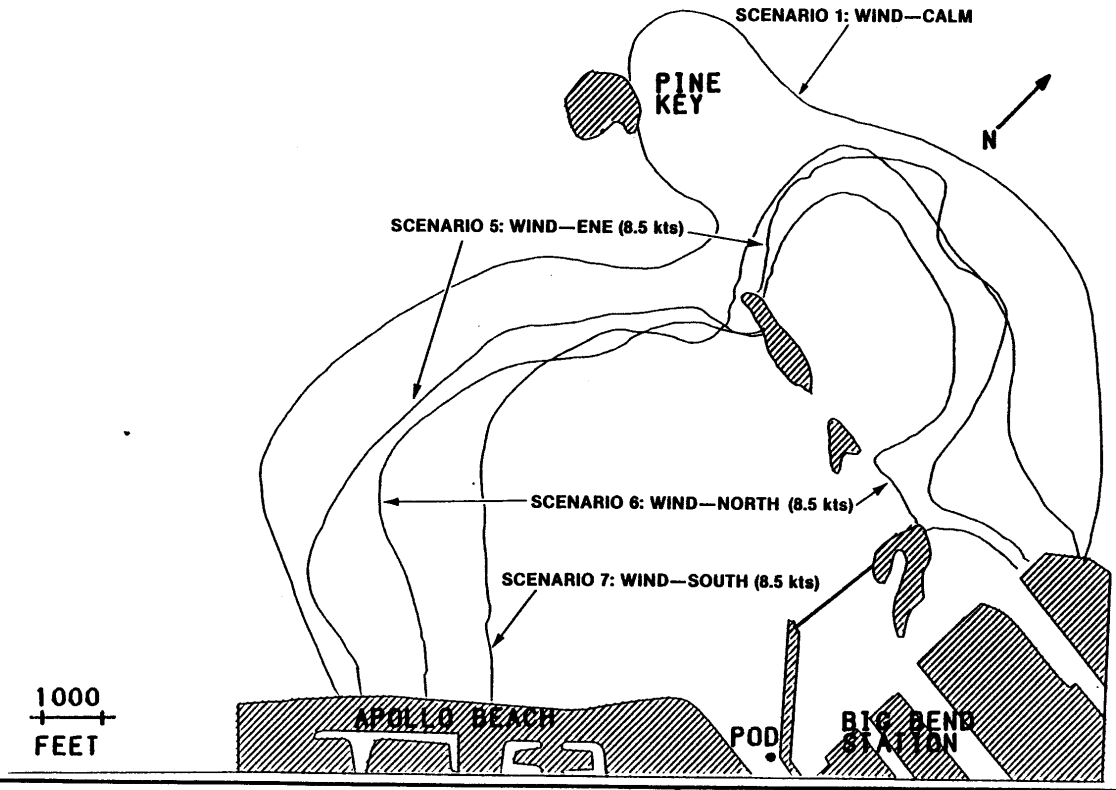

Figure 6-16
EFFECT OF WIND AT HIGH SLACK

SOURCE: ESE, 1984.

TAMPA ELECTRIC COMPANY

shown in Table 6-2, the neap tide (semi-diurnal, range 1.4 ft) produces a 26-percent smaller plume area. The spring tide (diurnal, range 2.8 ft) is only 3 percent less than the normal tide (diurnal, range 2.3 ft). Figures 6-17 and 6-18 show these three scenarios for low and high water slack, respectively.

The normal tide, the tide used for Scenarios 1 through 8, produces the greatest mixing zone area.

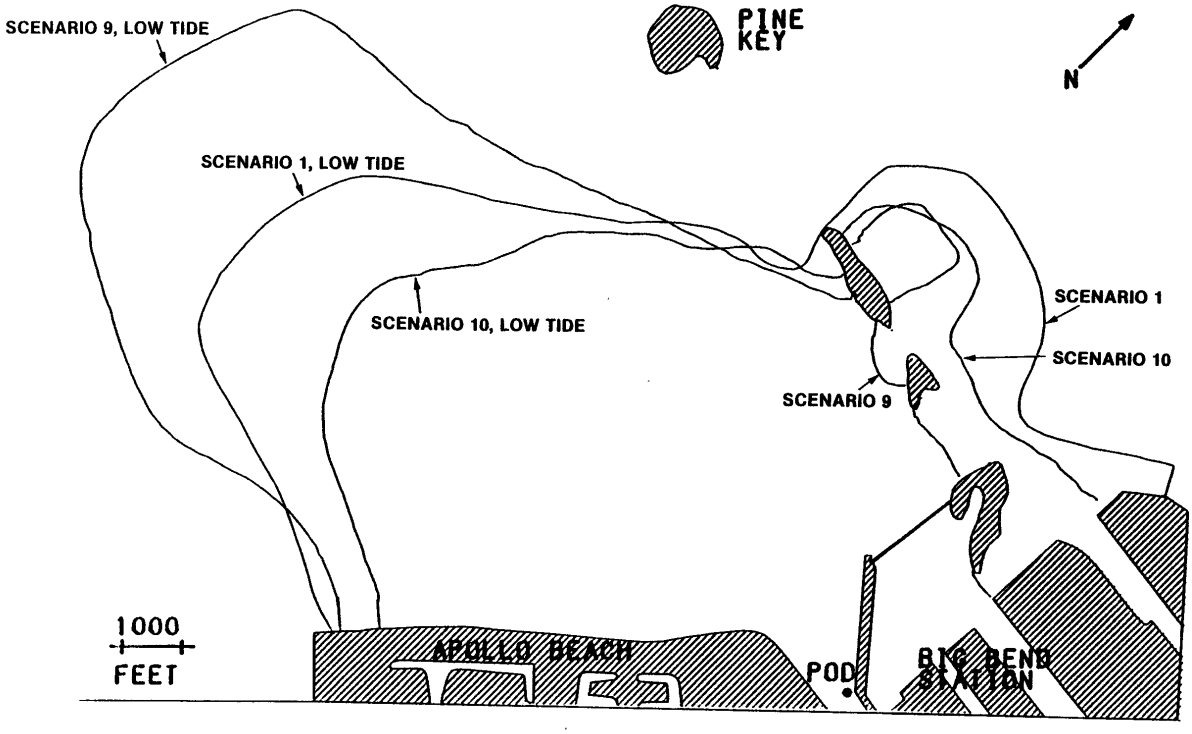

Figure 6-17
EFFECT OF TIDAL RANGE AT LOW SLACK

SOURCE: ESE, 1984.

TAMPA ELECTRIC COMPANY

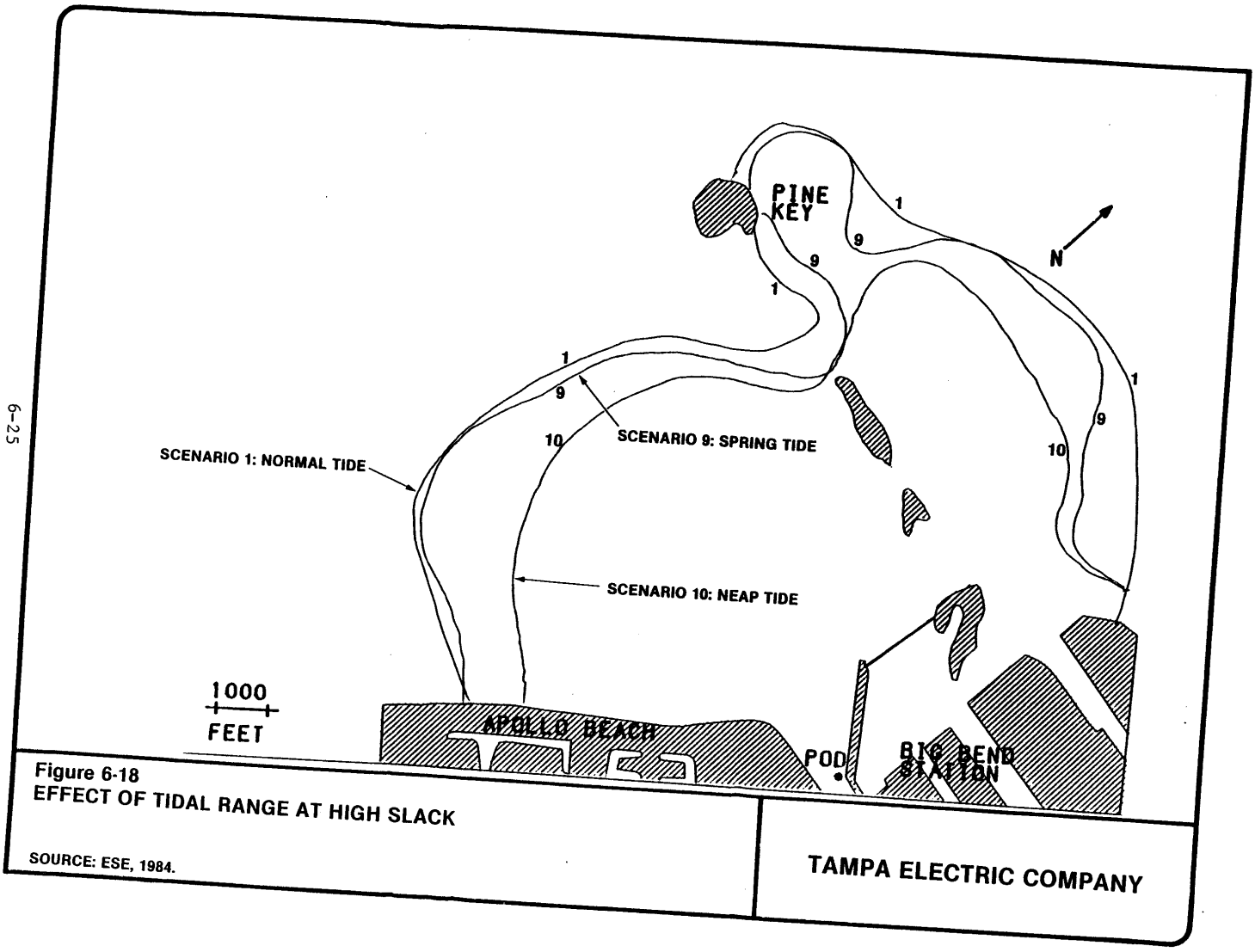

Figure 6-18
EFFECT OF TIDAL RANGE AT HIGH SLACK

SOURCE: ESE, 1984.

TAMPA ELECTRIC COMPANY

7.0 CONCLUSIONS

The CAFE-1/DISPER-1 models were calibrated to reproduce hydraulic and thermal mixing zone characteristics of Hillsborough Bay in the vicinity of the Big Bend Power Station. The hydraulic performance of CAFE-1 was verified versus tide and current meter data during a time period independent of the calibration period. Both tides and currents were simulated realistically during the verification time period. The ability of the CAFE-1/DISPER-1 models to reproduce thermal mixing zone size was verified during a thermal verification period independent of all prior calibration and verification periods. The average modeled thermal mixing zone area for all calibration and verification periods was 3 to 5 percent larger than the average of the observed plumes. An analysis of model accuracy indicates that instantaneous thermal mixing zone areas under four-unit operation can be predicted to be within about 18 percent of actual instantaneous plume areas.

The calibrated and verified model was used to predict thermal mixing zone area for 10 combinations of receiving water, meteorological, and power plant operating conditions (scenarios). The scenarios were designed to focus on extreme conditions which would tend to maximize thermal mixing zone area, while bracketing the range of conditions anticipated. Under typical environmental and discharge conditions, the thermal mixing zone area ranged from 1,200 to 2,900 acres. The largest thermal mixing zone area predicted under any of the extreme conditions was 4,539 acres, which is less than the prescribed permit condition of 4,980 acres. Thus, this study validates the size of the permitted mixing zone.

BIBLIOGRAPHY

Aquatec, Inc. 1979. Hydrothermal Field Study Report Big Bend Power Station, Tampa Bay, Florida.

Bowden, K.F. 1977. Turbulent Processes in Estuaries. In: Estuaries, Geophysics, and the Environment, National Academy of Sciences, Washington, D.C.

Chow, V.T. 1959. Open-Channel Hydraulics. McGraw-Hill Book Company, New York.

Divers, A.B. 1980. Thermal Infrared Survey, Big Bend Electric Station, Tampa, Florida, November 14-17, 1979. EPA Office of Research and Development, Las Vegas, Nevada.

Dronkers, J.J. 1964. Tidal Computations in Rivers and Coastal Waters.

Edinger, J.E., Brady, D.K., and Geyer, J.C. 1974. Heat Exchange and Transport in the Environment. Electric Power Research Institute, Report No. 14.

Leimkuhler, W., Connor, J., Wang, J., Christodoulou, G., and Sundgren, S. 1975. Two-dimensional Finite Element Dispersion Model. In: Modeling 75: Symposium on Modeling Techniques, V. II., ASCE, New York.

Murthy, C.R. and Okubo, A. 1977. Interpretation of Diffusion Characteristics of Oceans and Lakes Appropriate for Numerical Modeling. In: Manuscript Report Series No. 43, Symposium on Modeling of Transport Mechanisms in Oceans and Lakes. Burlington, Ontario, Canada, October 6-8, 1975.

Officer, C.B. 1977. Longitudinal Circulation and Mixing Relations in Estuaries. In: Estuaries, Geophysics, and the Environment, National Academy of Sciences, Washington, D.C.

Pritchard, D.W. 1971. Two-dimensional Models. In: Estuarine Modeling: An Assessment. G.H. Ward and W.H. Espey (Editors), NTIS PB-206-807.

Tampa Electric Company (TECO). 1980. 316 Demonstration Big Bend Station--Unit 4, Tampa, Florida.

Tampa Electric Company (TEC). 1984. Plan of Study for the Big Bend Unit 4 Thermal Mixing Zone Validation Study. Tampa, Florida.

Wang, J.D. 1978. Verification of Finite Element Hydrodynamic Model CAFE in Verification of Mathematical and Physical Models in Hydraulic Engineering. Proceedings of the 26th Annual Hydraulics Division Specialty Conference, College Park, Maryland, August 9-11, 1978.

BIBLIOGRAPHY
(Continued, Page 2 of 2)

Wang, J.D. 1983. Personal Communication with W.A. Tucker, December 7, 1983.

Wang, J.D. and Connor, J.J. 1975. Mathematical Modeling of Near Coastal Circulation. R.M. Parsons Laboratory for Water Resources and Hydrodynamics, Technical Report 200, Massachusetts Institute of Technology, Cambridge, Massachusetts.

Yudelson, J.M. 1967. A Survey of Ocean Diffusion Studies and Data. Tech. Memo 67-2, W.M. Keck Laboratory of Hydraulics and Water Resource, California Institute of Technology, Pasadena, California.